



US005143713A

**United States Patent** [19]

Phillips et al.

[11] Patent Number: **5,143,713**[45] Date of Patent: **Sep. 1, 1992**[54] **99MTC LABELED LIPOSOMES**

[75] Inventors: William T. Phillips; Robert W. Klipper, both of San Antonio, Tex.; James H. Timmons, Tacoma, Wash.; Alan S. Rudolph, Bowie, Md.

[73] Assignees: Board of Regents, The University of Texas System, Austin, Tex.; The United States of America as represented by the Secretary of the Navy, Washington, D.C.

[21] Appl. No.: 610,204

[22] Filed: Nov. 5, 1990

**Related U.S. Application Data**

[63] Continuation-in-part of Ser. No. 530,847, May 30, 1990.

[51] Int. Cl.<sup>5</sup> ..... A61K 43/00; A61K 49/02; A61K 9/127

[52] U.S. Cl. .... 424/1.1; 534/10; 534/14; 424/450; 428/402.2; 435/7.24

[58] Field of Search ..... 424/1.1, 450; 534/10, 534/14

[56] **References Cited****U.S. PATENT DOCUMENTS**

4,335,095 6/1982 Kelly ..... 424/9  
 4,452,774 6/1984 Jones et al. .... 424/1.1  
 4,615,876 10/1986 Troutner et al. .... 424/1.1  
 4,707,544 11/1987 Jones et al. .... 424/1.1 X  
 4,735,793 4/1988 Jones et al. .... 424/1.1  
 4,789,736 12/1988 Canning et al. .... 424/1.1 X  
 4,826,961 4/1989 Jones et al. .... 424/1.1 X  
 4,911,929 3/1990 Farmer et al. .... 424/450  
 4,925,650 11/1988 Nosco et al. .... 424/1.1  
 4,935,223 6/1990 Phillips ..... 424/1.1  
 4,938,947 7/1990 Nicolau et al. .... 424/1.1  
 5,019,369 5/1991 Presant et al. .... 424/1.1  
 5,049,391 9/1991 Suzuki et al. .... 424/450

**OTHER PUBLICATIONS**

Atsushi Takeda et al., "Intensification of Tumor Affinity of <sup>99m</sup>Tc-DL-Homocysteine by Cooperative Use of SH-containing Compounds", Nucl. Med. Biol., vol. 16, No. 6, pp. 581-585, 1989.

Claire De Labriolle-Vaylet et al., "Morphological and

Functional Status of Leukocytes Labelled with <sup>99m</sup>Tc-Technetium HMPAO", Radiolabelled Cellular Blood Elements, pp. 119-129.

Laurence Guilloteau et al., "Recruitment of <sup>99m</sup>Tc-Technetium- or <sup>111</sup>Indium-Labelled Polymorphonuclear Leucocytes in Experimentally Induced Polygranulomas in Lambs", J. of Leukocyte Bio., vol. 48, pp. 343-352, (1990).

Dialog Search Report.

Karl J. Hwang, "Liposome Pharmacokinetics," In: Liposomes from Biophysics to Therapeutics (M. J. Ostro, Ed.), pp. 109-156 (Marcel Dekker, Inc.) New York 1987.

Caride and Sostman, "Methodological Considerations for the Use of Liposomes in Diagnostic Imaging," Liposome Technology, vol. II:107-124 (1984).

Barratt et al., "The Labeling of Liposomal Membranes with Radioactive Technetium," Liposome Technology vol. II:93-106 (1984).

Beaumier and Hwang, "An Efficient Method for Loading Indium-111 into Liposomes Using Acetylacetone," J. of Nucl. Med. 23(9):810-815.

(List continued on next page.)

Primary Examiner—Richard D. Lovering

Assistant Examiner—John M. Covert

Attorney, Agent, or Firm—Arnold, White & Durkee

[57] **ABSTRACT**

The invention relates to the efficient preparation of radionuclide labeled liposomes and radionuclide-labeled liposome-encapsulated protein. In particular, a <sup>99m</sup>Tc carrier is used to label preformed liposomes or liposome-encapsulated hemoglobin. <sup>99m</sup>Tc-labeled liposomes and liposome-encapsulated <sup>99m</sup>Tc labeled hemoglobin are highly stable in vitro and in vivo and are suitable for a variety of clinical uses, including biodistribution imaging studies. The invention also relates to a method of labeling neutrophils using <sup>99m</sup>technetium-labeled liposomes or liposome-encapsulated hemoglobin. A kit method useful for the convenient preparation of <sup>99m</sup>Tc-labeled liposomes or liposome-encapsulated hemoglobin for clinical use is also disclosed.

31 Claims, 8 Drawing Sheets

## OTHER PUBLICATIONS

- Caride, Vincente J. "Technical and Biological Considerations on the Use of Radio-labeled Liposomes for Diagnostic Imaging," *Nucl. Med. Biol.* 17(1):35-39 (1990).
- Turner et al., "In-111-labeled liposomes: Dosimetry and Tumor Depiction," *Radiology* 166:761-765 (1988).
- Proffitt et al., "Tumor-Imaging Potential of Liposomes Loaded with In-111-NTA: Biodistribution in Mice," *J. of Nucl. Med.* 24(1):45-51 (1983).
- Hnatowich et al., "Labeling of Preformed Liposomes with Ga-67 and Tc-99m by Chelation," *J. of Nucl. Med.* 22(9):810-814 (1981).
- Love et al., "Effect of liposome surface charge on the stability of technetium ( $^{99m}\text{Tc}$ ) radiolabelled liposomes," *J. Microencapsulation* 6(1):105-113 (1989).
- O'Sullivan et al., "Inflammatory joint disease: a comparison of liposome scanning, bone scanning, and radiography," *Annals of the Rheumatic Diseases* 47:485-491 (1988).
- Williams et al., "Synovial accumulation of technetium labelled liposomes in rheumatoid arthritis," *Annals of the Rheumatic Diseases* 46:314-318 (1987).
- Morgan et al., "Localisation of experimental staphylococcal abscesses by  $^{99m}\text{Tc}$ -technetium-labelled liposomes," *J. Med. Microbiol.* 14:213-217 (1981).
- Eisenhut, M. "Radiopharmaka für die szintigraphische Tumordiagnostik," supplied by National Library of Medicine.
- Osborne et al., "Radionuclide-Labelled Liposomes—A New Lymph Node Imaging Agent," *Int'l J. of Nucl. Med. and Biol.* 6:75-83 (1979).
- Yu Bao-fa et al., "A New Lymph Node Imaging Agent- $^{99m}\text{Tc}$ -polyphase Liposome Oleatis ( $^{99m}\text{Tc}$ -plo)," *J. Oncol. (China)* 10:270-273 (1988).
- Farr et al., " $^{99m}\text{Tc}$  as a marker of liposomal deposition and clearance in the human lung," *Int'l J. of Pharmaceutics* 26:303-316 (1985).
- Palmer et al., "The Mechanism of Liposome Accumulation in Infarction," *Biochemica et Biophysica Acta* 797:363-368 (1984).
- Callahan et al., "A Modified Method for the In Vivo Labeling of Red Blood Cells with Tc-99m: Concise Communication," *J. Nucl. Med.* 23:315-318 (1982).
- Dewanjee, M. K. "Binding of  $^{99m}\text{Tc}$  Ion to Hemoglobin" *J. of Nuclear Medicine* 15(8):703-706 (1974).
- Delicostantinos et al., "Interaction of  $^{99m}\text{Tc}$ -Labeled Liposomes With Walker Tumor Cell In Vitro. Liposome-Mediated Introduction of Thalblastine Into Resistant Walker Tumor Cells" *Gen. Pharmac.* 14(4):407-411 (1983).
- Nakamura et al., "The behavior of  $^{99m}\text{Tc}$ -hexamethylpropyleneamineoxime ( $^{99m}\text{Tc}$ -HMPAO) in blood and brain" *Eur. J. Nucl. Med.* 15:100-107 (1989).
- Unger et al., "Gadolinium-DTPA Liposomes as a Potential MRI Contrast Agent Work in Progress" *Investigative Radiology* 23(12):928-932 (1988).
- Seltzer, S. E. "The Role of Liposomes in Diagnostic Imaging" *Radiology* 171(1):19-21 (1989).
- Article in *Radiology Today*, Mar. 1989 "Indium-labeled liposomes effectively target secondary tumors" p. 3.
- Article by Lang, Letters to the Editor, *J. Nucl. Med.*, 31(6):1115 (1990).
- Article by Ballinger, Letters to the Editor, *J. Nucl. Med.*, 31(6):1116 (1990).
- Article by Ballinger et al., "Technetium-99m HM-PAO Stereoisomers: Differences in Interaction with Glutathione," *J. Nucl. Med.*, 29(12):1998-2000 (1988).

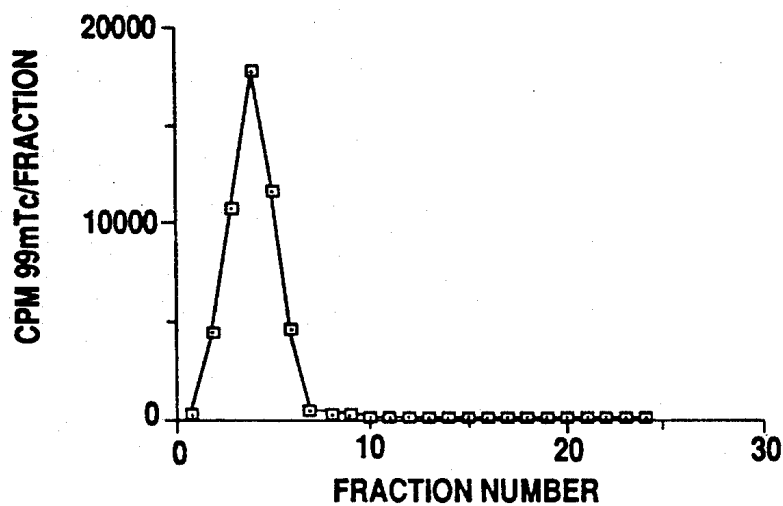


Fig. 1

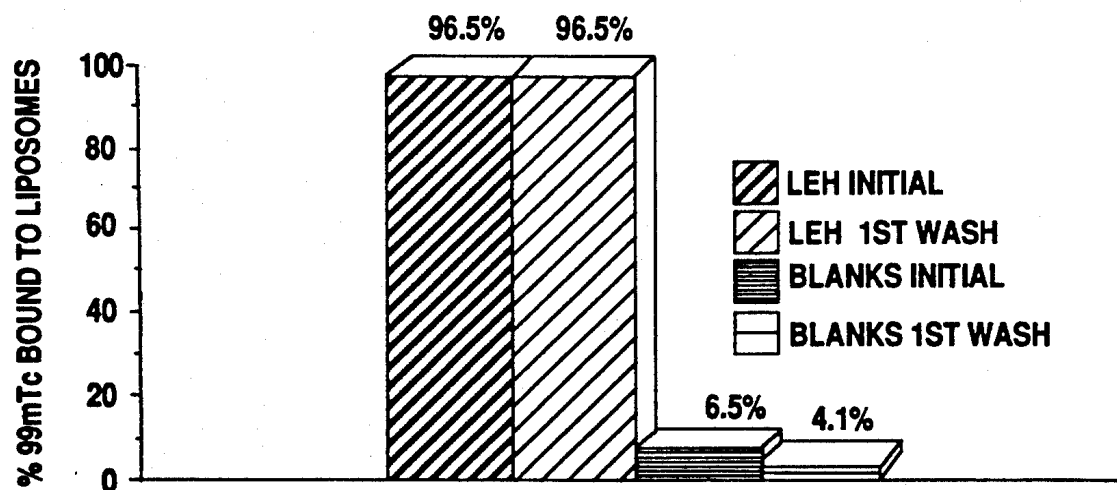


Fig. 2

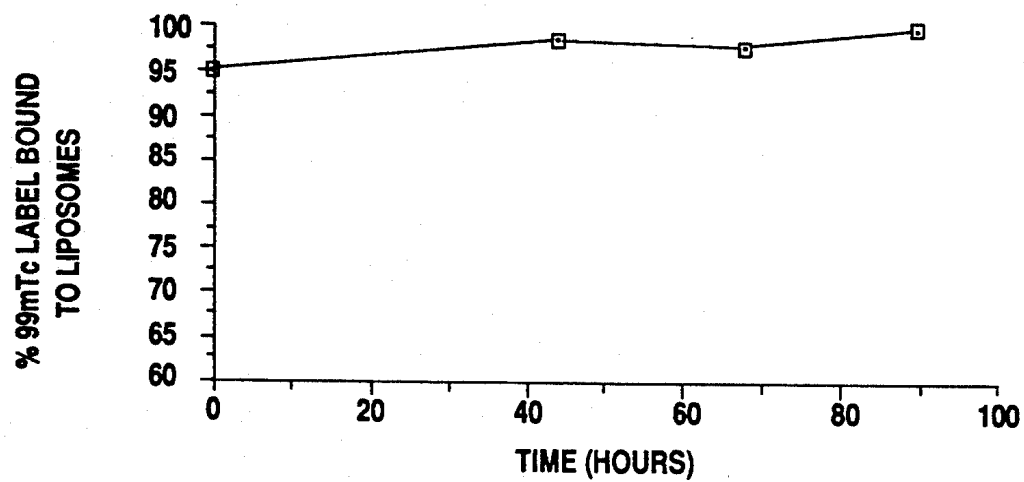


FIG. 3

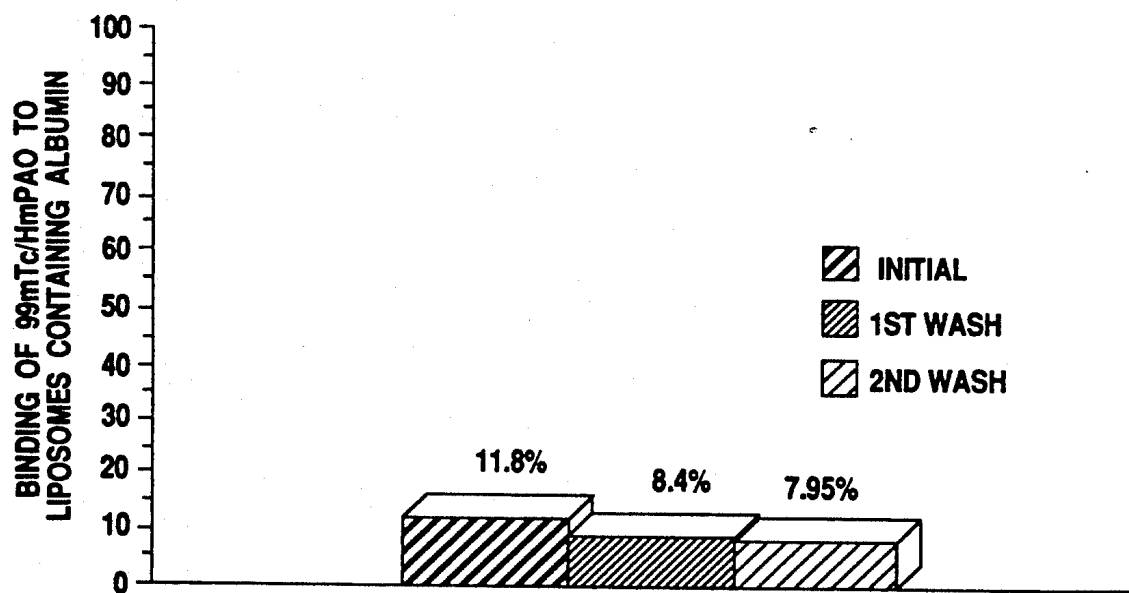


Fig. 4

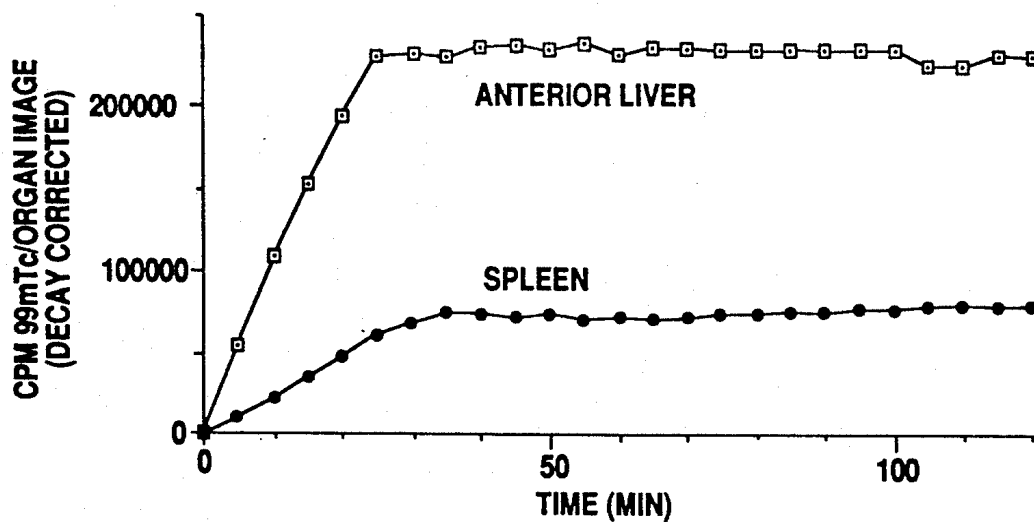


Fig. 5A

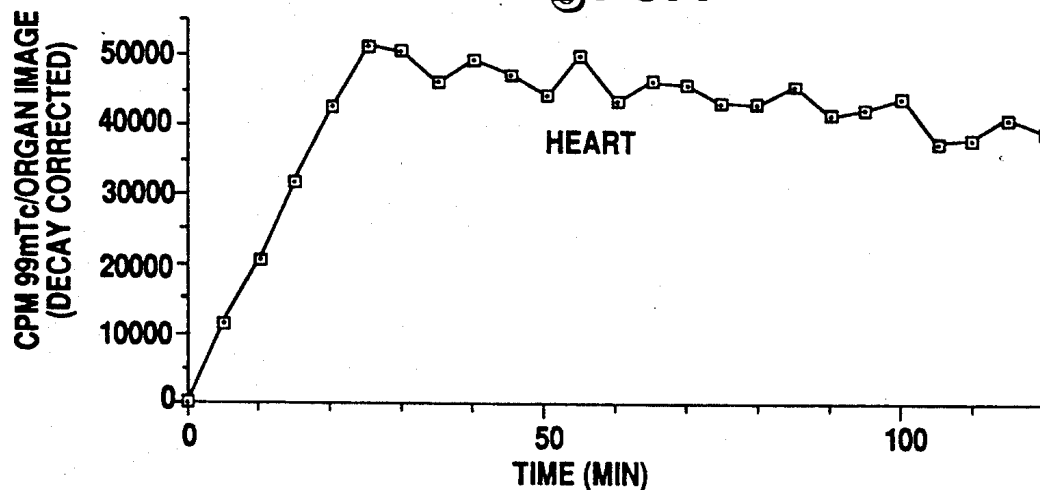


Fig. 5B

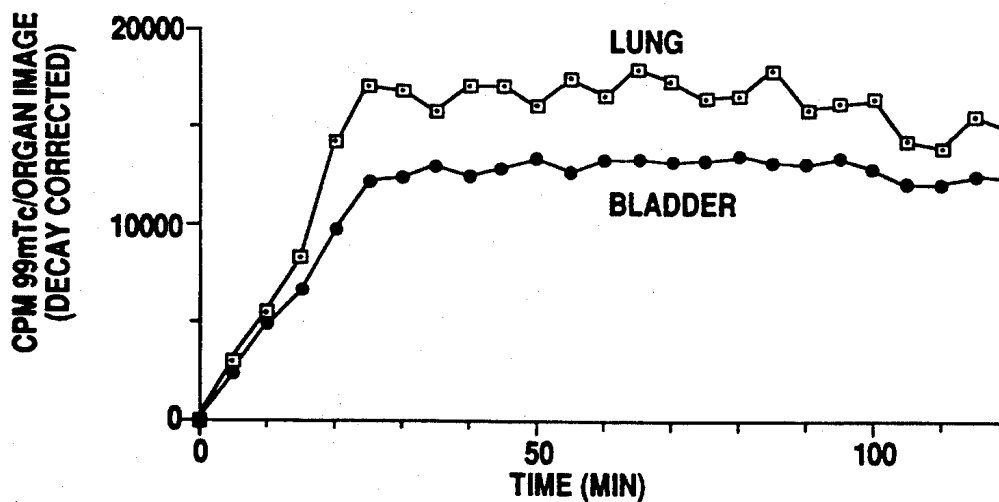
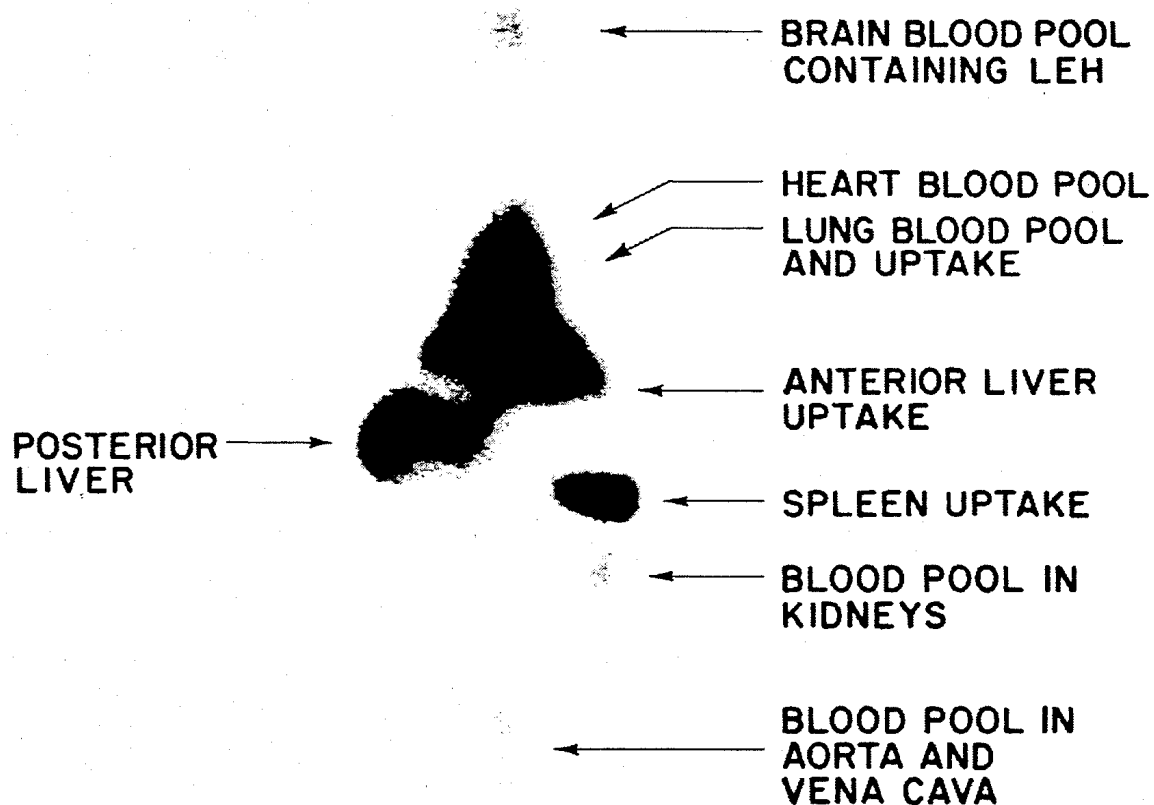


Fig. 5C

**FIG. 6**

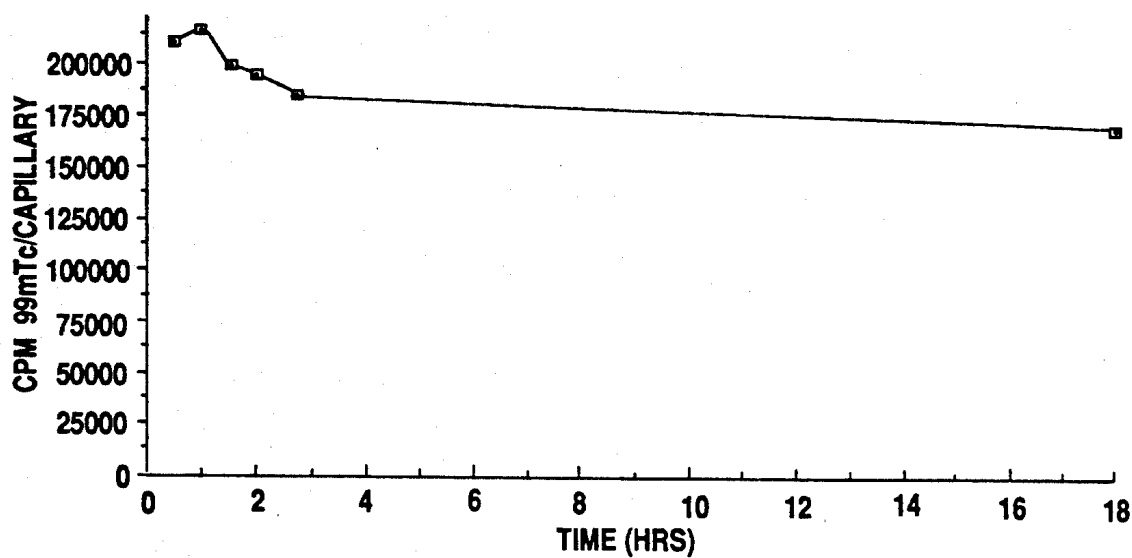


Fig. 7

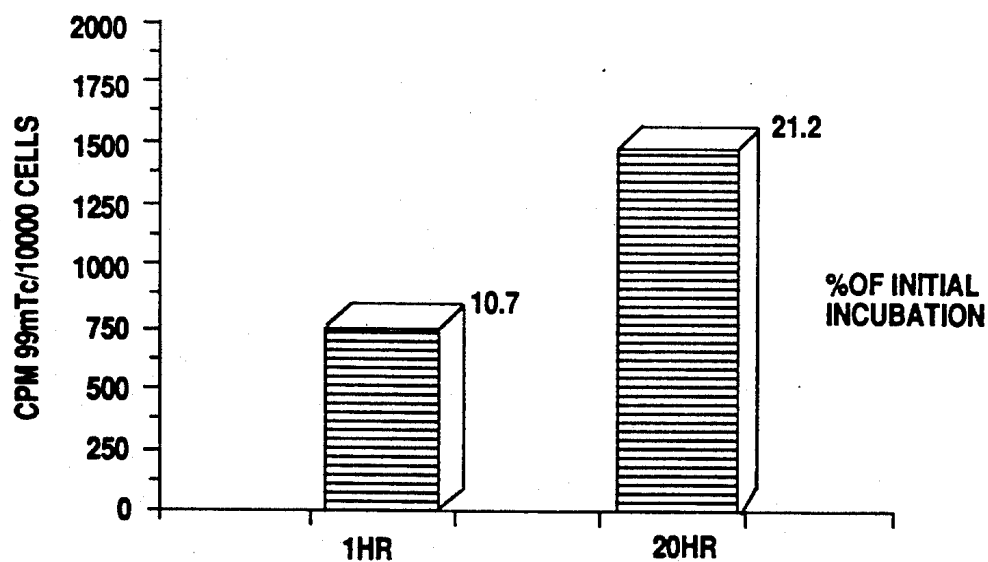


Fig. 8

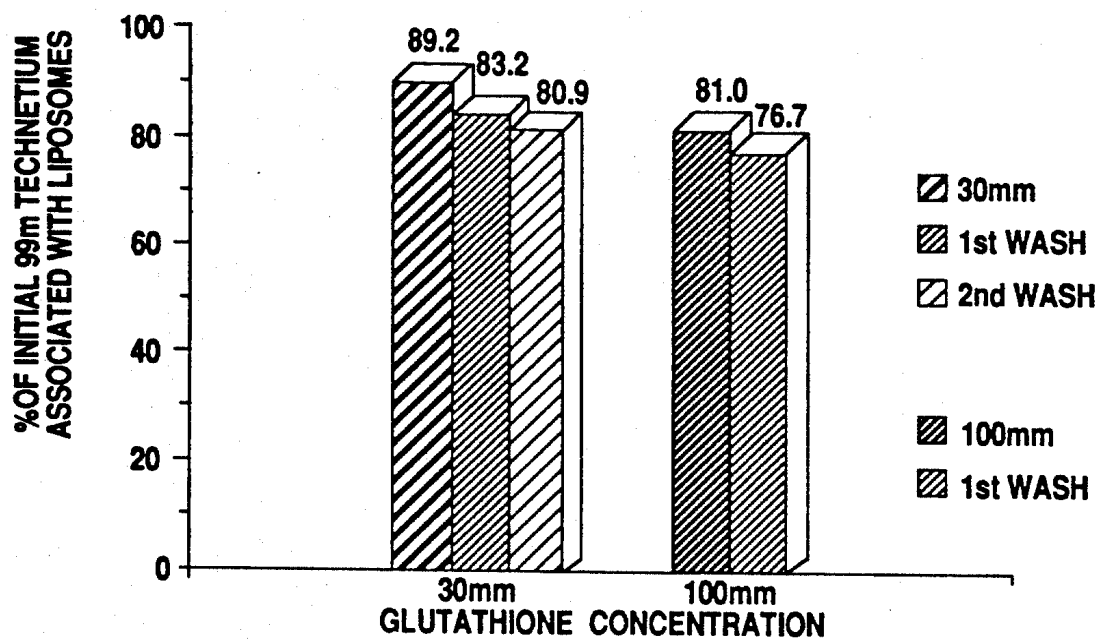
IN VITRO STABILITY OF  $^{99m}$  TECHNETIUM  
LABELING OF LIPOSOMES

Fig. 9

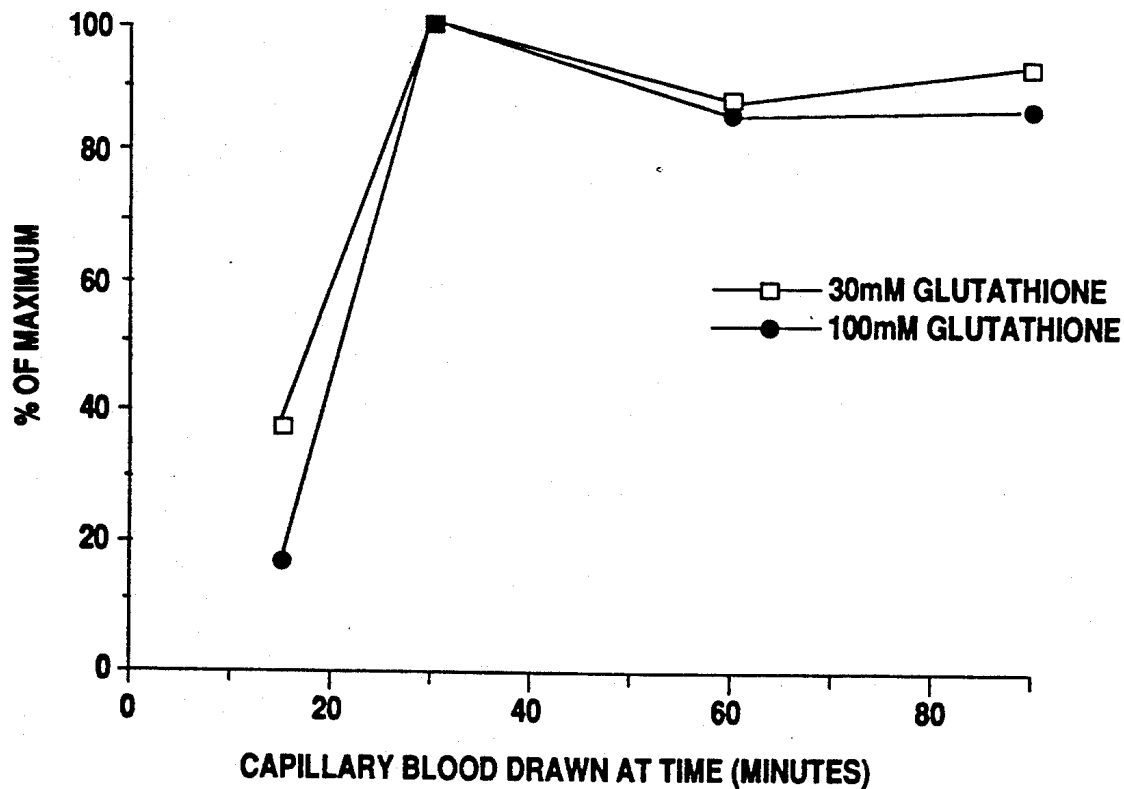
IN VIVO STABILITY OF  $^{99m}$  TECHNETIUM-  
LABELED LIPOSOMES CONTAINING GSH

Fig. 10



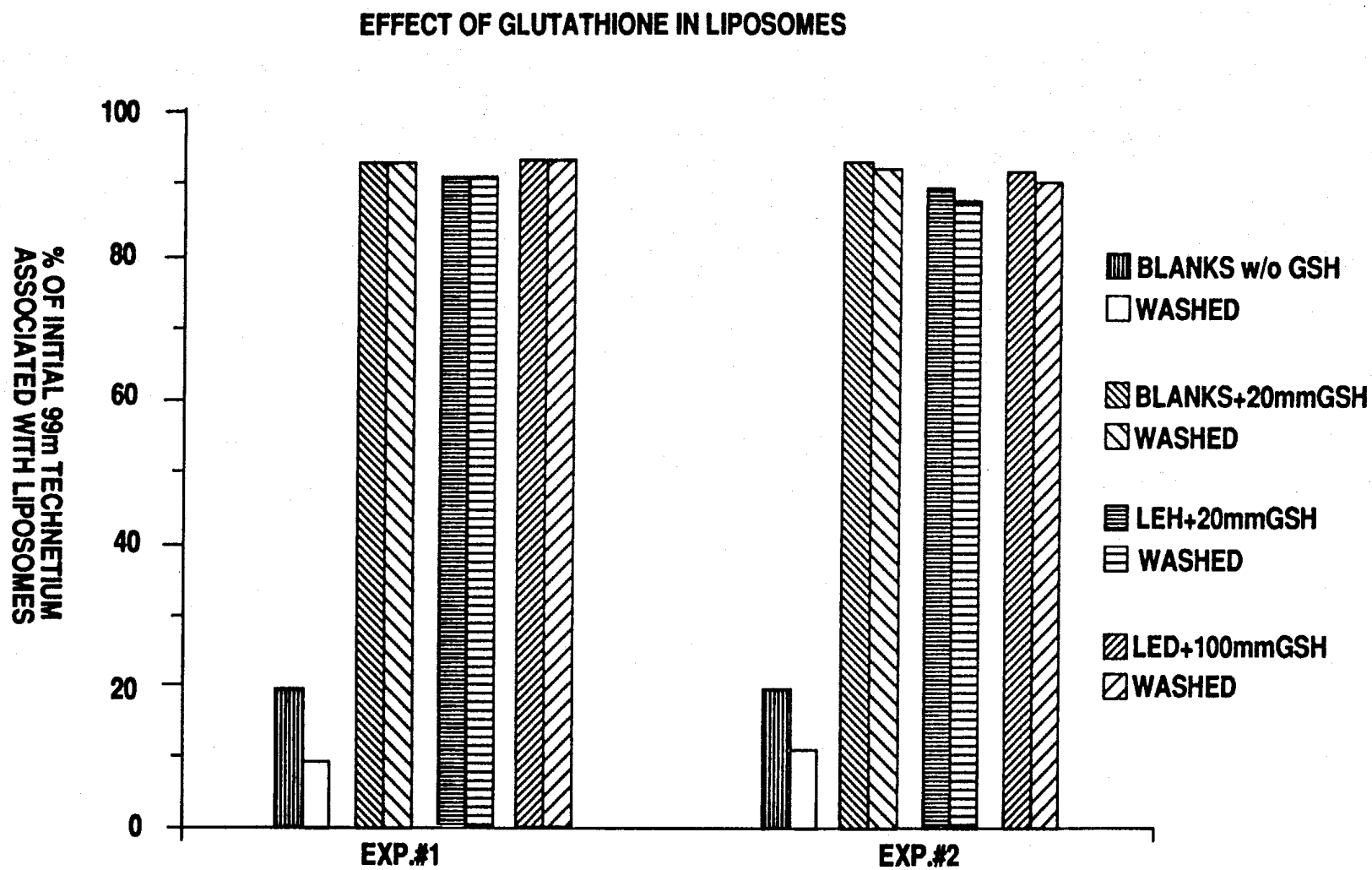


Fig. 11

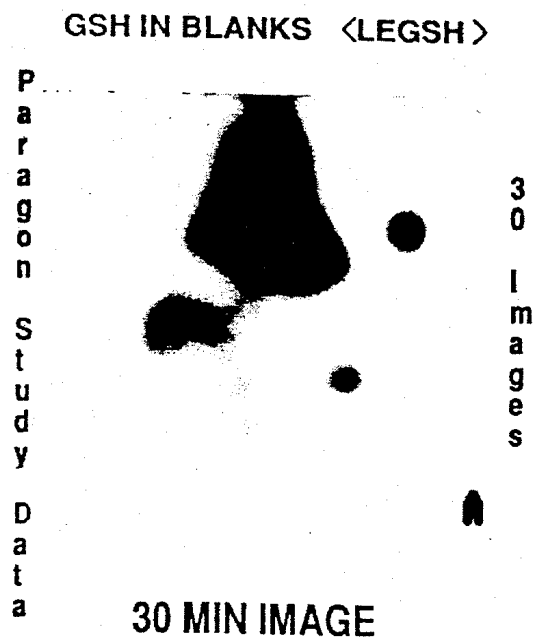


Fig. 12A

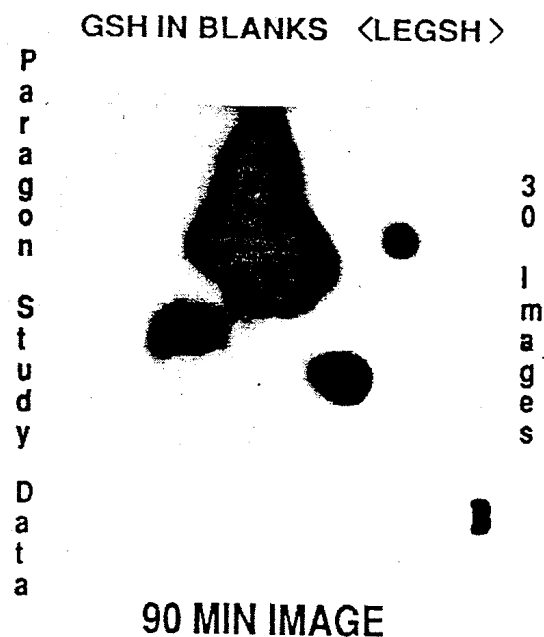


Fig. 12B

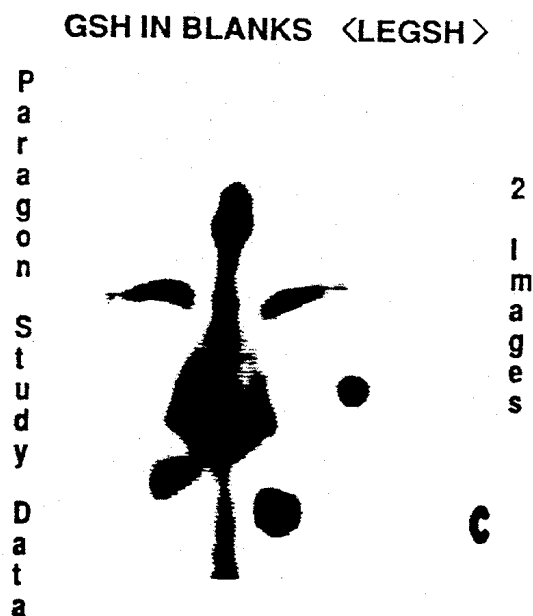


Fig. 12C

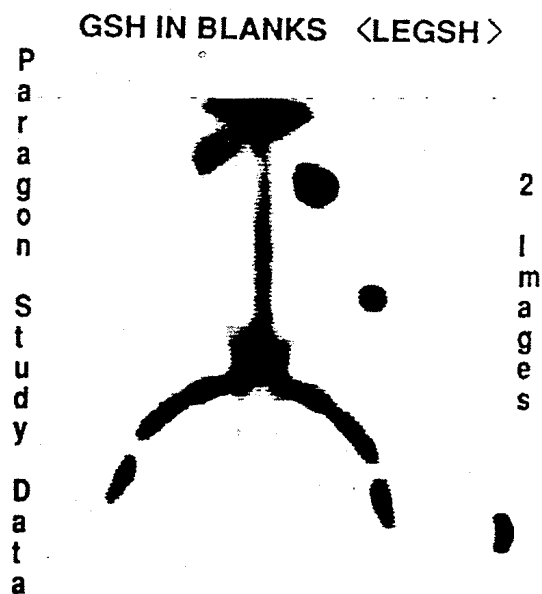


Fig. 12D

## 99MTC LABELED LIPOSOMES

The U.S. Government may have certain rights in the present invention pursuant to the terms of Grant No. N 00014-89-K-0077 awarded by the Office of Naval Research.

This is a continuation-in-part of U.S. patent application Ser. No. 07/530,847, filed May 30, 1990.

## BACKGROUND OF THE INVENTION

## 1. Field of the Invention

The invention relates to a rapid and highly efficient method of labeling liposomes and liposome-encapsulated protein. In particular, the method relates to radionuclide labeling of preformed liposomes with or without encapsulated protein by means of a radionuclide carrier characterized as being membrane diffusible.

Table 1 is a list of abbreviations used.

TABLE 1

cpm	counts per minute
DTPA	diethylenetriaminepenta-acetic acid
GBq	gigabequerels
HMPAO	hexamethylenepropylene amine oxime
LEH	liposome-encapsulated hemoglobin
PBS	phosphate buffered saline
PYP	pyrophosphate
Tc	Technetium
LUV	large unilamellar vesicles

## 2. Description of Related Art

Liposomes are of considerable interest because of their value as carriers for diagnostic agents, particularly radiopharmaceuticals for tracer and imaging studies. Successful biodistribution studies, for example, require attachment of a radiolabel to the liposome. Unfortunately, the entrapment of water soluble radionuclides within the liposome is relatively inefficient. Another major problem in using liposomes is their leakiness, resulting in limited usefulness for many applications (Hwang, K. J., in *Liposomes from Biophysics to Therapeutics*, M. J. Ostro, Ed., Marcel Dekker, N.Y., 1987).

Radioactive markers have been widely used as a non-invasive method for studying the distribution of drugs in vivo. The use of gamma emitting radioisotopes is particularly advantageous because, unlike beta-emitters, they can easily be counted in a scintillation well counter and do not require tissue homogenization prior to counting. In addition, gamma-emitters can be imaged with nuclear gamma cameras. With this type of imaging, the dynamic biodistribution can be followed non-invasively using consecutive one minute computer acquired scintigraphic images which are analyzed to calculate organ biodistribution curves.

The most common radiolabel used in diagnostic radiopharmaceuticals today is  $^{99m}\text{Tc}$ . This radionuclide is produced from the beta decay of  $^{99}\text{molybdenum}$  and has a half-life of 6 hours. It is widely available from a generator system at low cost and its relatively short half-life provides for safer and more convenient handling than other available radionuclides. Its gamma emission is in the range of 140 Kev which is an ideal range for producing high resolution images (Caride, V. J. and Sostman, H. D. in *Liposome Technology*, Vol. II, G. Gregoriadis, Ed., CRC Press, Boca Raton, 1984). Heptavalent  $^{99m}\text{TcO}_4^-$  is produced from the generator and since it is relatively unreactive, must be reduced to a lower oxidation state before use as a radiopharmaceu-

tical. Stannous chloride is the most commonly used reducing agent (Barratt, G. M., Tuzel, N. S. and Ryman, B. E. in *Liposome Technology*, Vol. II, G. Gregoriadis, Ed., CRC Press, Boca Raton, 1984).

Radiolabeled complexes have been employed as a means for labeling liposomes. Isonitrile radionuclide complexes of Tc and other gamma-emitters appear to have use for labeling vesicles with lipid membranes, including red blood cells (U.S. Pat. No. 4,452,774, Jones et al., Jun. 5, 1984). Propylene amine oxime complexes with  $^{99m}\text{Tc}$  are stable neutral lipophilic complexes which have been approved for radioimaging in vivo as an adjunct in the detection of altered regional cerebral perfusion (Ceretec <sup>TM</sup>). These complexes which diffuse across cellular walls have been shown to localize in red blood cells, although radioactivity is readily washed from the cells. (U.S. Pat. No. 4,789,736, Canning et al., Dec. 6, 1988 and U.S. Pat. No. 4,615,876, Troutner et al., Oct. 7, 1986). Furthermore, the usefulness of these complexes is limited because the complexes are not stable. Ceretec <sup>TM</sup>, for example, has a useful life of approximately 30 minutes.

The radionuclide of  $^{111}\text{indium}$  ( $^{111}\text{In}$ ) has found some use as an imaging agent. Multilamellar lipid vesicles labeled with  $^{111}\text{In}$  using 8-hydroxyquinoline showed a labeling efficiency of 30% (Caride, V. J. and Sostman, H. D. in *Liposome Technology*, Vol. II, G. Gregoriadis, Ed., CRC Press, Boca Raton, 1984). Higher labeling efficiencies have been shown for loading  $^{111}\text{In}$  into the aqueous compartment of liposomes. Acetylacetone, a water soluble lipophilic chelator, can be complexed with  $^{111}\text{In}$ . This is then mixed with liposome-encapsulated nitrilotriacetic acid with subsequent formation of labeled nitrilotriacetic acid. The resulting labeled liposomes are unstable unless excess acetylacetone is removed by an ion exchange process (Beaumier, P. L. and Hwang, K. J., *J. Nucl. Med.*, 23, 810-815 (1982)).

In general, labeling efficiency of 50-70% for  $^{99m}\text{Tc}$  has been reported for multilamellar vesicles and 4-20% for small unilamellar vesicles when using stannous chloride to reduce the pertechnetate. A persistent problem in all these methods is the removal of excess reducing agent as well as elimination of free pertechnetate. Separation can be done by gel filtration or dialysis, but there is often formation of a  $^{99m}\text{Tc}$ -tin chloride colloid which is not readily distinguishable or separable from the liposomes (Barratt, G. M., Tuzel, N. S. and Ryman, B. E. in *Liposome Technology*, Vol. II, G. Gregoriadis, Ed., CRC Press, Boca Raton, 1984). This confounds the results of biodistribution studies since interpretation may be subject to altered uptake influenced by the labeled colloidal tin.

Attempts at labeling liposomes with imaging radio-tracers have produced variable results (Barratt, G. M., Tuzel, N. S. and Ruman, B. E. in *Liposome Technology*, Vol. II, G. Gregoriadis, Ed., CRC Press, Boca Raton, 1984; Caride, V. J. and Sostman, H. D. in *Lipid Technology*, Vol. II, G. Gregoriadis, Ed., CRC Press, Boca Raton, 1984; Caride, V. J., *Nucl. Med. Biol.*, 17, 35-39 (1990); Hwang, K. J. in *Liposomes from Biophysics to Therapeutics*, M. J. Ostro, Ed., Marcel Dekker, Inc., N.Y., 1987). Many radioisotope labels weakly bind to liposomes resulting in inaccurate biodistribution data. A more efficient imaging label procedure uses  $^{111}\text{indium}$  chloride ( $^{111}\text{InCl}$ ) and nitrilotriacetic acid, a metal chelator (Beaumier, P. L. and Hwang, K. J., *J. Nucl. Med.*, 23, 810-815 (1982); Turner, A. F., Presant, C. A.,

Proffitt, R. T., Williams, L. E., Winsor, D. W., Werner, J. L., *Radiology*, 166, 761-765 (1988); Proffitt, R. T., Williams, L. E., Presant, C. A., Tin, G. W., Uliana, J. A., Gamble, R. C. and Baldeschwieler, J. D., *J. Nucl. Med.*, 24, 45-51 (1983). The nitrilotriacetic acid is incorporated into the liposome during the manufacturing process. The preformed liposomes are then incubated for 30 minutes with  $^{111}\text{InCl}$ . Although the  $^{111}\text{InCl}$  nitrilotriacetic acid labeling method has proven to be effective and the label tightly attached to the liposome, a heating step ( $60^\circ\text{C}$ ) is required, which adds to the time and inconvenience involved in the preparation. In a clinical situation convenience and speed are important. A further consideration is the expense of the  $^{111}\text{In}$  radionuclide. The present cost of  $^{111}\text{In}$  is approximately \$135/mCi while cost of  $^{99m}\text{Tc}$ , a superior imaging agent, is \$0.35/mCi. This difference is highly significant in determining cost of imaging procedures to the patient and in a decision by the health provider to offer such services.

Other labeling carriers have been tried. Small amounts of octadecylamine-DTPA in liposomes have been shown to rapidly label the liposomes with  $^{67}\text{Ga}$  or  $^{99m}\text{Tc}$  by chelation with efficient labeling, but over 30% of the label is lost after a 2 hour incubation in plasma (Hnatowich, D. J., Friedman, B., Clancy, and Novak, M. J. *Nucl. Med.*, 22, 810-814 (1981)).

The reasons for instability of  $^{99m}\text{Tc}$  labeled liposomes are not well understood, although instability may be related to the liposome surface charge. Recent work has shown that the in vitro methods currently used to assess the stability of labeled liposomes do not predict isotope stability in vivo, and that the nature of the binding between the isotope and the liposome surface is important in regulating in vivo isotope stability (Love, W. G., Amos, N., Williams, B. D., and Kellaway, I. W., *J. Microencapsulation*, 6, 103-113 (1989)). The result is that even when labeling methods appeared to be highly efficient, and little instability was demonstrated in plasma or serum, significant loss of label could occur when the labeled liposomes were introduced into an animal or human.

Despite attempts to develop stable  $^{99m}\text{Tc}$ -labeled liposomes, there has been little success. In a thoroughly detailed review of liposomal labeling with radioactive technetium, Barratt et al. noted that technetium labeling techniques vary widely in efficiency. Moreover, stability is generally recognized to be poor, especially in vivo. Most methods of labeling liposomes with  $^{99m}\text{Tc}$  encapsulate the  $^{99m}\text{Tc}$  during liposome manufacture. However, these encapsulation methods do not solve the problem of in vivo dissociation of  $^{99m}\text{Tc}$  from the liposome. The dissociated  $^{99m}\text{Tc}$  is usually visualized in the kidneys and bladder. These problems clearly illustrate that development of a reliable method to load high levels of  $^{99m}\text{Tc}$  into liposomes without in vivo dissociation would be beneficial in view of the many clinical uses for radiolabeled liposomes (Hwang, K. J. in *Liposomes from Biophysics to Therapeutics*, M. J. Ostro, Ed., Marcel Dekker, N.Y., 1987).

There are numerous clinical applications for  $^{99m}\text{Tc}$ -liposomes. Comparison studies of liposome scanning, bone scanning and radiography have been performed in inflammatory joint disease. Liposome scans have been shown to be positive only in clinically active inflammatory disease. The method has also been able to discriminate between different grades of joint tenderness, in contrast to bone scans (O'Sullivan, M. M., Powell, N.,

French, A. P., Williams, K. E., Morgan, J. R., and Williams, B. D., *Ann. Rheum. Dis.*, 47, 485-491, 1988; Williams, B. D., O'Sullivan, M. M., Saggu, G. S., et al., *Ann. Rheum. Dis. (UK)*, 46, 314-318 (1987)). Other studies include the localization of abscesses (Morgan, J. R., Williams, K. E., Davies, R. L., et al., *J. Med. Microbiol.*, 14, 213-217 (1981); tumor scanning (Eisenhut, M., *Therapiewoche (West Germany)* 30, 3319-3325 (1980); lymph node imaging (Osborne, M. P., Richardson, V. J., Jeyasingh, K., Ryman, B. E., *Int. J. Nucl. Med. Biol. (England)* 6, 75-83 (1979); Yu, B., *Chin. J. Oncol. (China)* 10, 270-273 (1988); clearance in the human lung (Farr, S. J., Kellaway, I. W., Parry-Jones, D. R., Woolfrey, S. G., *Int. J. Pharm. (Netherlands)* 26, 303-316 (1985)); and infarction (Palmer, T. N., Caride, V. J., Caldecourt, M. A., Twickler, J., and Abdullah, V., *Biochim. Biophys. Acta* 797, 363-368 (1984)).

Other potential uses of a liposome label include cardiac gated blood pool angiography and gastrointestinal bleeding detection. The most commonly used process known as the modified in vivo technique is fairly lengthy and requires 2-3 injections into the patient. For red blood cell labeling, the patient is injected with 1-2 mg of stannous PYP (Callahan, R. J., et al., *J. Nuclear Medicine* 23, 315-318 (1982)). Fifteen minutes later a blood sample is withdrawn and incubated with  $^{99m}\text{TcO}_4^-$  (free pertechnetate). The patient is then reinjected with the radiolabeled blood, the whole procedure requiring up to 1 hour. The major disadvantage of this technique is that the label is often poor and free pertechnetate is taken up in the stomach, resulting in intestinal contamination and making the results difficult to interpret. A rapid labeling technique would very likely alleviate this major problem, allowing improved cardiac and gastrointestinal bleeding detection imaging.

There is a distinct need for radiopharmaceutical materials that can be broadly applied to clinical applications and to biodistribution and bioimaging studies.  $^{99m}\text{Tc}$  labeled liposomes would appear to be an ideal reagent but present methods of labeling liposomes with  $^{99m}\text{Tc}$  are generally inefficient. A far greater problem is the lack of in vivo stability of  $^{99m}\text{Tc}$  labeled liposomes, thereby limiting their use and creating uncertainty in interpretation of results.

The present invention is the surprising discovery that incubation of encapsulated reducing agent with liposomes, radionuclide labeled liposomes having high in vivo stability can be readily and efficiently prepared. The liposomes, preferably labeled with  $^{99m}\text{Tc}$ , are useful in a wide range of clinical applications related to biodistribution and imaging. Labeled liposome-encapsulated protein may also be prepared by this method and has also been shown to have high stability in vivo.

#### SUMMARY OF THE INVENTION

Stable  $^{99m}\text{Tc}$ -labeled liposomes and  $^{99m}\text{Tc}$  labeled liposome-encapsulated protein and their novel method of preparation are the subject of the present invention. The method of preparation results in over 95% labeling efficiency and produces labeled liposomes that are surprisingly stable in vivo for relatively long periods of time. The labeled liposomes are excellent imaging agents.

Labeled liposomes (LL) may be prepared by incubating liposomes with a label, generally a radionuclide, in the form of a complex which acts as a carrier for the label. It has been found that labeling is surprisingly efficient when the incubating is performed in the pres-

ence of an antioxidant compound. The antioxidant compound may be present in the incubation mixture of labeled carrier and liposomes, but is most preferably incorporated within the liposome prior to incubation with the label carrier.

Liposome-encapsulated labeled protein (LELP) may also be prepared by this method in a manner analogous to that of labeled liposome preparation. Liposome-encapsulated protein having an antioxidant present within the liposome is incubated with a label carrier complex until liposome-encapsulated labeled protein is formed. It is not known to what extent the label should be membrane diffusible, although it appears that some lipophilic character is desirable and that the carrier is significantly associated with the membrane.

After incubation, excess labeled carrier and antioxidant may be washed from the LL or LELP. Since the labeling is so efficient, only a few percent of the initial radioactivity is found in the wash. In cases where the carrier and antioxidant are relatively innocuous, the washing is optional and the labeled liposomes may be used directly after incubation. This would be the case, for example, when the antioxidant is glutathione and the carrier is HMPAO. If separation is desired, centrifugation at 10–20,000  $\times g$  may be used or, a rapid and convenient separation may be effected with a syringe pack column attached to the syringe containing the labeled liposomes. The liposomes will pass in the void volume while any free radionuclide, pertechnetate for example, would be retained on the column. In a most preferred labeling procedure for clinical use, a freeze dried preparation of  $^{99m}\text{Tc}$ -HMPAO is reconstituted with  $^{99m}\text{TcO}_4^-$  and immediately incubated at room temperature with liposomes or liposome-encapsulated hemoglobin for a period as short as 5 minutes prior to use in a patient. Washing is not necessary.

In a novel aspect of the invention, it has been discovered that labeling is highly efficient when an antioxidant is encapsulated within preformed liposomes or liposome-encapsulated protein. Liposomes to be labeled may be first incubated with the antioxidant. This antioxidant/liposome mixture may then be washed, removing excess antioxidant not attached to the liposome surface. These prepared liposomes may then be incubated with the labeled carrier. Although the antioxidant may be added to the incubation mixture with liposomes or liposome-encapsulated protein, washed and then added to the label carrier, this procedure provides liposomal preparations that are less stable in vivo. This is so even though the initial labeling efficiency is quite high. Most preferably the antioxidant compound is an inorganic or organic reducing agent, for example  $\text{Sn}^{+2}$  or glutathione. Compounds with free sulfhydryl appear to be suitable, for example, cysteine, although compounds of general structure  $\text{RSH}$  where R is an alkyl group or other organic moiety capable of interaction with a liposome would also be expected to work. Relatively large moieties such as proteins may also function well, particularly enzymes such as superoxide dismutase, catalase or met-hemoglobin reductase. Ascorbic acid also induced efficient binding of the label within the liposome. The mechanism of this action is not known, particularly whether or not the antioxidant agent is involved in the binding. It is possible, at least in the case of a  $^{99m}\text{Tc}$ -HMPAO, that presence of a reducing agent converts lipophilic  $^{99m}\text{Tc}$ -HMPAO to a hydrophilic form that becomes trapped inside the liposome. In any event, binding affinity of  $^{99m}\text{Tc}$  to liposomes or to LEH is

relatively inefficient without antioxidant present. In earlier experiments, it was found that binding of the label was very efficient when LEH preparations obtained from Naval Research Laboratories (Washington, DC) were used, but labeling was poor when LEH was prepared as described in Example 1 but without glutathione or ascorbic acid. It was later found that where efficient labeling was achieved, glutathione had been present in the preparations.

Both the liposomes and the protein encapsulated within the liposome have binding affinity for the label. The precise type of interaction is not known except to say that an antioxidant such as glutathione was found to be necessary to keep the label tightly bound with the liposome, regardless of the presence of a protein.

The protein encapsulated in the liposomes is preferably hemoglobin, although other proteins binding to selected labels could be chosen. Encapsulation of substances within liposomes is well-known and techniques for encapsulation have been described (Hwang, K. J. in *Liposomes from Biophysics to Therapeutics*, M. J. Ostro, Ed., Marcel Dekker, Inc., New York, 1987). In particular, a method for encapsulating hemoglobin in liposomes has been described (Farmer et al., U.S. Pat. No. 4,911,929, Mar. 27, 1990). Hemoglobin appears to be preferred as the encapsulated protein because in its presence  $^{99m}\text{Tc}$ , presently the most widely used radionuclide in nuclear medicine, is tightly bound within the liposome (Barratt, G. M., Tuzel, N. S. and Ryman, B. E. in *Liposome Technology*, Vol. II, G. Gregoriadis, Ed., CRC Press, Boca Raton, 1984). Nevertheless, there may be instances in which other labels would be desired for specific studies or clinical purposes and thus a different protein might change the binding properties of the label. Certain beta-emitters, for example, might be desired and such radionuclides might bind more or less tightly in the presence of albumin or another protein. On the other hand, in certain applications, increased disassociation of the label may be desirable, as in instances where the liposome is intended to deposit the label at target organs or body areas. The label would then be dispensed at the target area. In any event, it is contemplated that the protein encapsulated may be chosen with consideration of the desired effect. Suitable proteins might include transferring, myoglobin, myosin, insulin, globulin, casein, keratin, lectin, ferritin and elastin. In addition, certain fragments or subunits of proteins might also be useful, including the  $\beta$ -chain of hemoglobin.

Denaturated as well as native proteins could be encapsulated within liposomes and used to bind a label. Partially denatured proteins might be useful as well, particularly if more binding sites are exposed.

Several types of labels could be used of which radionuclides would be the most useful for medical applications. Examples of beta-emitters include  $^{32}\text{P}$ ,  $^{35}\text{S}$ ,  $^{36}\text{Cl}$ ,  $^{24}\text{Na}$ ,  $^{32}\text{K}$  and  $^{45}\text{Ca}$ . Positron-emitters such as  $^{68}\text{Ga}$ ,  $^{82}\text{Rb}$ ,  $^{22}\text{Na}$ ,  $^{75}\text{Br}$ ,  $^{122}\text{I}$  and  $^{18}\text{F}$  would be useful in computerized tomographic studies. Of particular interest are the gamma-emitting radionuclides, for example,  $^{24}\text{Na}$ ,  $^{51}\text{Cr}$ ,  $^{59}\text{Fe}$ ,  $^{67}\text{Ga}$ ,  $^{86}\text{Rb}$ ,  $^{99m}\text{Tc}$ ,  $^{111}\text{In}$ ,  $^{125}\text{I}$  and  $^{195}\text{Pt}$ .  $^{99m}\text{Tc}$  and  $^{111}\text{In}$  have been found particularly useful for imaging studies in human subjects.

In the incubation of liposomes or liposome-encapsulated protein with a labeled carrier, the carrier must be capable of complexing with the desired radionuclide and also diffusing through the liposomal membrane. Generally this will require a carrier that is lipophilic and also sufficiently water soluble to permit efficient

transfer within the water compartment of the lipid vesicle. For the radionuclide  $^{99m}\text{Tc}$ , the preferred carrier is hexamethylenepropylene amine oxime. This carrier transports the metal across the bilayer membrane of the liposome and, presumably, may subsequently transfer  $^{99m}\text{Tc}$  to the liposome, to the encapsulated protein or may become entrapped as the undissociated hydrophilic-converted carrier complex.

It will be recognized that a preferred carrier will depend to some extent on the lipid composition and surface charge of the liposome which can be positive, negative or neutral. A preferred carrier is HMPAO. This carrier readily crosses the membrane of negatively charged liposomes. Other carriers could be chosen on their ability to complex with the selected radionuclide and the efficiency of transport across the liposomal membrane to mediate exchange with the encapsulated capture material.

Furthermore, special ligands on the liposome surface, oligosaccharides or immunoglobulins for example, could also affect uptake of the carrier as well as targeting of the liposomes within the body. The synthesis of liposomes with charged or neutral surfaces having a wide variety of compositions is well known in the art. The selection of the appropriate liposome would require some experimentation and would depend on the carrier chosen and in turn on the radionuclide required.

The labeling efficiency of this method is greater than 90% and stability in vivo is quite high, as indicated in the examples. After more than 18 hours, 70% of the injected liposome-encapsulated  $^{99m}\text{Tc}$  labeled hemoglobin was recovered in vivo from rabbit blood (FIG. 7). An in vivo experiment with  $^{99m}\text{Tc}$  labeled liposomes indicated that up to 96% of the initial label remained associated with the liposomes after 1.5 hr, (FIG. 10). No other method has reported this high stability in vivo. In fact, the present invention has overcome one of the most significant disadvantages in the use of  $^{99m}\text{Tc}$  as a radiolabeling agent, i.e., the apparent release of free technetium in vivo, therefore casting doubt that the radioimages are representative of intact liposomes (Barratt, G. M., Tuzel, N. S. and Ryman, B. E. in *Liposome Technology*, Vol. II, G. Gregoriadis, Ed., CRC Press, Boca Raton, 1984)).

The present invention also contemplates the use of  $^{99m}\text{Tc}$  labeled liposomes or liposome-encapsulated labeled hemoglobin in kit form. Thus, in a preferred mode of use, freeze dried liposomes or liposome-encapsulated hemoglobin would be incubated with a radionuclide carrier, such as  $^{99m}\text{Tc}$  hexamethylenepropylene amine oxime, before administration to patients or experimental animals. Other radionuclides could be used as could other encapsulated proteins besides hemoglobin, for example albumin, as described in Example 2.

Example 4 illustrates the use of  $^{99m}\text{Tc}$  labeled liposome-encapsulated hemoglobin in biodistribution studies, but it will be appreciated that appropriate carriers could be used to transfer other gamma emitters to capture agents within a liposome. For example,  $^{111}\text{In}$ ,  $^{125}\text{I}$  and  $^{67}\text{Ga}$ . The method could also be applied to beta- or positron emitters; for example,  $^{32}\text{P}$ ,  $^{35}\text{S}$  or, in the latter category,  $^{68}\text{Ga}$  and  $^{18}\text{F}$ . The distribution of the label can be detected by means appropriate to the emitter. Gamma emitters are commonly detected using well established scintillation counting methods or nuclear gamma cameras. Beta emitters can be detected by radiation detection devices specific for beta particles while

positron emitters are determined using various designs of a positron emission tomography apparatus.

Likewise, the general method described in the present invention would be particularly applicable to magnetic resonance imaging, simply by preparing a paramagnetically labeled liposome or liposome-encapsulated carrier molecule, administering the labeled liposome in vivo and determining the distribution of the paramagnetic label. The usual means for determining paramagnetic species is nuclear magnetic resonance detection. Bone marrow imaging has been shown particularly useful with  $^{99m}\text{Tc}$  labeled liposomes which demonstrate a large amount of bone marrow uptake from the circulation several hours after administration (FIG. 12).  $^{99m}\text{Tc}$  labeled liposomes having an average size of about 0.05–0.1  $\mu$  appear to be most useful for this purpose. Larger liposomes would be expected to image in different areas, for example, the lungs or other organs. Clearly, one could expect to image different regions of the body by using different size ranges of labeled liposome preparations.

In another aspect of the invention,  $^{99m}\text{Tc}$  labeled LEH is used to label neutrophils. Neutrophils incubated with labeled liposomes apparently phagocytized the labeled liposomes and became labeled with  $^{99m}\text{Tc}$ . The 20% labeling achieved shows promise for developing a highly stable neutrophil label. This method could be used to achieve similar labeling with any phagocytized cell, for example monocytes or other cells that are capable of engulfing a labeled liposome. This could be controlled to some extent by the size and composition of the liposome employed.

#### BRIEF DESCRIPTION OF THE DRAWINGS

FIG. 1 is a graph showing the fractionation of liposome-encapsulated  $^{99m}\text{Tc}$  labeled liposomes on a Sephadex G-200 column 70 hours after binding of the label to the encapsulated hemoglobin. All the  $^{99m}\text{Tc}$  is associated with the liposomal fraction.

FIG. 2 shows the percent  $^{99m}\text{Tc}$  binding initially to liposomes using HMPAO where LEH is liposome-encapsulated hemoglobin and blanks are liposomes without encapsulated material. There is no loss of the  $^{99m}\text{Tc}$  label during the first wash.

FIG. 3 shows the in vitro stability of  $^{99m}\text{Tc}$  labeled liposomes in lactated Ringers solution at 2° C.

FIG. 4 shows 11.8% initial binding of  $^{99m}\text{Tc}$  to liposome-encapsulated albumin.

FIG. 5 shows time activity curves acquired from imaging data of the heart, liver, spleen, bladder and lung of a rabbit injected with  $^{99m}\text{Tc}$  labeled LEH.

FIG. 6 shows various anatomical features seen on the image of a New Zealand rabbit infused with  $^{99m}\text{Tc}$ -labeled LEH acquired at 2 hours labeling.

FIG. 7 is a graph of  $^{99m}\text{Tc}$  radioactive counts of capillaries drawn serially after infusion of 25 milliliters of  $^{99m}\text{Tc}$ -labeled LEH at a concentration of 50 mg total lipid per milliliter into a 2 kilogram New Zealand rabbit.

FIG. 8 shows the labeling of neutrophils incubated with  $^{99m}\text{Tc}$  labeled liposome-encapsulated hemoglobin. The radioactivity labeling efficiency of the neutrophils is 10.7% after 1 hour of incubation and 21.1% after 20 hours of incubation.

FIG. 9 shows the in vitro stability of  $^{99m}\text{Tc}$ -labeled liposomes prepared using liposomes encapsulating 30 mM or 100 mM glutathione.

FIG. 10 shows the in vivo stability of  $^{99m}\text{Tc}$ -labeled liposomes prepared from liposomes containing 30 mM

or 100 mM glutathione. Labeled liposomes preparations were injected into rabbits and blood samples taken at the times indicated.

FIG. 11 is a chart comparing  $^{99m}\text{Tc}$ -labeling efficiency and effect of washing on blank liposomes, liposomes encapsulating 20 mM glutathione, and liposome-encapsulated hemoglobin also entrapping either 20 mM glutathione or 100 mM glutathione.

FIG. 12 is a gamma scintillation image of a rabbit after administration of  $^{99m}\text{Tc}$ -labeled liposomes containing glutathione. The four frames are different images of the same rabbit. The top frames show the middle body taken at 30 minutes and 90 minutes. The lower frames show the top of the body, frame C, and the lower body, frame D, images taken after 20 hours.

## DETAILED DESCRIPTION OF THE PREFERRED EMBODIMENTS

### Liposome-Encapsulated Protein

As discussed above, several different proteins as well as different liposomal compositions may be used to prepare liposomes and encapsulated labeled protein. Albumin is an example of a protein that can be encapsulated by the method described in Example 1 used to encapsulate hemoglobin. In a most preferred embodiment, hemoglobin is encapsulated in monolamellar negatively charged liposomes. Methods of producing liposome-encapsulated protein include a variety of methods, for example, reverse phase evaporation, homogenization and pressure extrusion. A method of producing liposome-encapsulated hemoglobin is described in Example 1. Other forms of hemoglobin can be substituted for bovine hemoglobin, including recombinant human hemoglobin. Well-known methods of encapsulation with liposomes could be employed to encapsulate proteins with special affinity for a desired label. The encapsulated protein need not be a native molecule or even the entire molecule. For example, only the  $\beta$ -chain of hemoglobin might be encapsulated. Examples of other proteins that could be encapsulated include transferrin, myoglobin, myosin, ferritin, globulin, insulin, elastin, keratin, casein, hemoglobin fragments and other polypeptides.

Efficient binding of the label within the liposome requires the presence of a reductant, thought to act as an antioxidant, preferably glutathione which is most preferably encapsulated with the liposome-encapsulated protein before incubation with a label carrier. If glutathione is added to the liposome after the protein is encapsulated, the final labeled product is efficiently labeled but appears not to have high in vivo stability.

### $^{99m}\text{Tc}$ -labeled Liposomes

The discovery of an efficient labeling method for liposomes resulting in labeled liposomes that are stable in vitro and in vivo solves one of the more important problems in liposome labeling. The method is illustrated with the use of  $^{99m}\text{Tc}$ -labeled HMPAO as a carrier to introduce the label into a preformed liposome. Glutathione, ascorbic acid or other suitable antioxidant is most preferably encapsulated within the liposome prior to incubation with a labeled carrier to achieve efficient labeling. Possibly glutathione or other reducing agents convert the  $^{99m}\text{Tc}$  HMPAO complex into a more hydrophilic form that is retained inside the liposome (Ballinger, J. R., Reid, R. H. and Gulenchyn, K. Y., J. Nucl. Med., 29, 1998-2000(1988); Lang, J. J., J. Nucl. Med.,

31, 1115 (1990); Ballinger, J., J. Nucl. Med., 31, 1115-1116 (1990)).

### $^{99m}\text{Tc}$ Carriers

The  $^{99m}\text{Tc}$  carrier found most preferable is an alkylene propylene amine oxime that complexes with  $^{99m}\text{Tc}$  and can be purchased as a lyophilized preparation (Ceretek TM, Amersham, Ill.). In this form, HMPAO is mixed with sterile eluate from a technetium  $^{99m}\text{Tc}$  generator. The generator eluate may be adjusted to a radioactive concentration of between 0.37-1.11 GBq (10-30 mCi) in 5 ml by dilution with preservative-free, non-bacteriostatic saline prior to mixing with 0.5 mg of HMPAO. The  $^{99m}\text{Tc}$  complex forms almost immediately and is then incubated with liposomes containing encapsulated reductant or liposome-encapsulated hemoglobin at room temperature for 5-15 minutes. Room temperature incubation is a significant advantage over other methods of liposome labeling presently used.  $^{111}\text{In}$ , for example, can be retained within liposome-encapsulated nitrilotriacetic acid but the encapsulated nitrilotriacetic acid must be incubated with  $^{111}\text{In}$  indium chloride at 60° C. for 30 minutes. Thus  $^{99m}\text{Tc}$  labeled liposomes prepared by the method of the present invention could be used in the assessment of in vivo distribution of new liposome drug agents that contain proteins or other heat labile drugs, whereas the heat required for the preparation of the  $^{111}\text{In}$  labeled liposome would denature or destroy any encapsulated heat sensitive material.

$^{99m}\text{Tc}$  liposomes also have potential in assessing the effectiveness of targeting with liposomes having antibodies attached to the surface. Antibodies to infectious agents or to tumor cells would bind to the targeted areas allowing radioimaging and possible delivery of drugs to the site.

### EXAMPLE 1

#### Preparation of Liposome-Encapsulated Hemoglobin

Liposome components are: distearoyl phosphatidylcholine (DSPC) (American Lecithin Company, Atlanta, Ga.), supplied as Phospholipid 100-H composed of 95% hydrogenated distearoyl phosphatidylcholine and up to 5% lysophosphatidylcholine; cholesterol (Calbiochem, San Diego, Calif.) at a purity of greater than 99% by TLC; and Dimyristoyl phosphatidyl DL-glycerol (DMPG) (Avanti Polar Lipids, Birmingham, Ala.) which was used without further purification. d-Alpha-tocopherol (Sigma, St. Louis, Miss.) was mixed in a 200 mg/ml solution in chloroform. All lipids were dried down from chloroform stock solutions in a mole ratio of 10:9:1 (DSPC:cholesterol:DMPG:alpha-tocopherol) and stored overnight in a vacuum desiccator to remove organic solvent. Samples were then rehydrated with solutions of trehalose (Pfanstiehl Laboratories, Waukegan, Ill.) in 30 mM phosphate buffered saline pH 7.4 and warmed in a water bath at 60° C. for one hour.

The resultant multilamellar vesicles formed from rehydration were reduced to large unilamellar vesicles (LUVs) using a high shear, high pressure apparatus (Microfluidics Corp., Boston, Mass.). The LUV's were then frozen in liquid nitrogen and lyophilized. The resultant dry sugar-lipid preparations were then hydrated with a solution of concentrated (25 g/ml) bovine hemoglobin (Hb) (Biopure Corp., Boston, Mass.) containing 30 mM or 100 mM glutathione or ascorbic acid and placed on an orbital shaker at 4° C. for 2 hours. These



solutions were then run through a microfluidizer to form LEH and centrifuged to remove extravesicular hemoglobin and reducing agent (14,000×g for 1 hour). The resulting LEH was concentrated by centrifugation and stored in the refrigerator at 4° C. or shell frozen using a bench top lyophilized.

#### EXAMPLE 2

##### <sup>99m</sup>Tc Labeling of Liposome-Encapsulated Hemoglobin

Liposome-encapsulated hemoglobin (prepared as described in Example 1 or purchased from Vestar, Inc., San Dimas, Calif. or Naval Research Laboratories, Washington, D.C.) was washed 3 times with phosphate buffered saline by centrifugation and resuspended with phosphate buffered saline to remove subcellular-sized debris and free hemoglobin. LEH containing glutathione or ascorbic acid was resuspended in PBS to yield a hematocrit value of approximately 50. <sup>99m</sup>Tc (10 mCi) in 5 ml sterile water for injection was used to reconstitute hexamethylenepropylene amine oxime (HMPAO) supplied as a freeze dried preparation (Cereteck™, Amersham, Arlington Heights, Ill.) for 5 min at room temperature. This mixture of <sup>99m</sup>Tc-HMPAO complex and glutathione was then incubated with LEH (10 mg -1000 mg total lipid dose of LEH containing 2.5-300 mg intravesicular hemoglobin) for 5 minutes with intermittent swirling after which the radio-labeled LEH was washed (centrifugation at 20,000 ×g for 30 minutes) with PBS and the labeling efficiency determined (bound to pellet/total). LEH was then resuspended to a constant lipid dose for injection.

Fractionation of <sup>99m</sup>Tc-labeled LEH on Sephadex G-200 70 hours after binding is shown in FIG. 1. The labeled LEH eluted with the void volume. There was insignificant detection of free <sup>99m</sup>Tc. FIG. 2 indicates that liposomes without hemoglobin (blanks) bound less than 10% of the <sup>99m</sup>Tc added to LEH preparations. The blanks were prepared as described in Example 1 for the preparation of LEH except that during hydration no hemoglobin or glutathione were added.

The <sup>99m</sup>Tc-labeled LEH exhibited excellent in vitro stability over a period of at least 90 hours storage in lactated Ringer's solution, as shown in FIG. 3 and in FIG. 9. FIG. 3 shows the stability of liposome-encapsulated labelled hemoglobin prepared from LEH purchased from Naval Research Laboratories and incubated with <sup>99m</sup>Tc-HMPAO without the addition of glutathione (glutathione is present as a result of the particular method of preparation of LEH). FIG. 9 shows the stability of liposome-encapsulated labelled hemoglobin prepared as described above with glutathione present at a concentration of 20 mM or 100 mM.

Liposome-encapsulated albumin was prepared as described for hemoglobin except that glutathione was omitted from the incubation mixture. Approximately 12% of the label carried by the <sup>99m</sup>Tc-HMPAO became bound to the encapsulated albumin. One-third of the label was removed after two washings with PBS (see FIG. 4).

#### EXAMPLE 3

##### <sup>99m</sup>Tc-labeled Liposomes

Liposomes prepared as described in Example 1 above or purchased from a commercial source (Vestar, San Dimas, Calif.) and containing 30 mM or 100 mM glutathione were incubated with <sup>99m</sup>Tc-HMPAO. The percent of initial <sup>99m</sup>Tc associated with the liposomes was

measured before and after washing and compared with the amount of label retained in liposome-encapsulated labeled hemoglobin. The results are shown in FIG. 9 and FIG. 11. There was virtually no loss of <sup>99m</sup>Tc label from liposomes or liposome-encapsulated hemoglobin prepared by incubating with <sup>99m</sup>Tc-HMPAO in the presence of glutathione. Labeling efficiency was less than 20% when glutathione was absent and there was a loss of almost 50% of the label after a single wash.

In vivo stability of <sup>99m</sup>Tc labeled liposomes was 85% and 90% respectively for liposomes incubated in the presence of 30 mM and 100 mM glutathione when tested over a period of 1.5 hr. (FIG. 10).

#### EXAMPLE 4

##### Animal Biodistribution Studies with <sup>99m</sup>Tc-labeled LEH

Young adult male New Zealand white rabbits (2.5-3.0 kg) were anesthetized intramuscularly with ketamine:xylazine at 50 mg/kg:10mg/kg respectively. While anesthetized, venous and arterial access lines were secured. The rabbit was then restrained in the supine position under a low energy, parallel hole collimator of a gamma camera and imaged for <sup>99m</sup>Tc activity at 140 Kev with a 20% window. Baseline blood samples were drawn and the metered (40 ml/kg/hr) injection of the LEH was begun. An aliquot of the injection material was reserved for lipid analysis and radioactive quantitation. Blood was then drawn at intervals to assess changes in blood chemistry, complete blood counts, the duration of LEH in the circulation and subsequent deposition and processing of the LEH by the organ systems. At 20 hours post-injection, the rabbit was sacrificed by anesthesia overdose and tissues recovered for quantitation and pathology study. Images acquired for the first two hours and at 20 hours were analyzed by drawing regions of interest around all organ systems (heart, lungs, anterior and posterior liver, spleen, kidneys, bladder and aorta) within the camera field of view. Counts in these regions of interest were calculated at 1 min interval for 20 hours and then a 20 hours. Counts were decay corrected to correct for radioactive decay. These data were entered into a MacIntosh computer for graphic demonstration of changes in biodistribution occurring with time as shown in FIG. 5. The levels of <sup>99m</sup>Tc distribution in the rabbit heart, liver, spleen and lungs are shown in FIG. 6. FIG. 12 shows the distribution of the label concentrated in the bone marrow 20 hours after administration.

The in vivo recovery of <sup>99m</sup>Tc-labelled LEH from rabbit blood over a period of 18 hours is shown in FIG. 7.

#### EXAMPLE 5

##### <sup>99m</sup>Tc-Labeling of Neutrophils

Sixty ml of whole blood was drawn and diluted with 3 volumes of Hanks Buffered Salt Solution. Neutrophils were isolated with Ficol Hypaque centrifugation at 600×g for 20 minutes. Recovered neutrophils were washed ×2 with a lymphocyte maintenance medium. The neutrophils were counted and 2 separate aliquots of 10<sup>7</sup> neutrophils were incubated with radiolabeled LEH for 1-20 hours at 37° C. The suspensions were counted and then centrifuged to yield a neutrophil pellet. The pellet was resuspended and washed ×2. The labeling efficiency was then determined (bound to white cell



pellet/total). As shown in FIG. 8, over 20% of the initial activity was incorporated by the neutrophils after 20 hours of incubation.

### EXAMPLE 6

#### Bone Marrow Imaging

Two rabbits were injected with  $^{99m}\text{Tc}$  labeled liposomes prepared as described in Example 3. Twenty hr after administration, images were taken on the whole animal using a gamma scintillation camera set at 140 KeV with a 20% window. As shown in FIG. 12, the majority of the radionuclide had left the circulation and was concentrated in the bone marrow.

The present invention has been described in terms of particular embodiments found by the inventors to comprise preferred modes of practice of the invention. It will be appreciated by those of skill in the art that in light of the in the particular embodiments exemplified without departing from the intended scope of the invention. For example, various modifications of the liposomal surfaces could be used to better target certain organs, or glutathione analogs or derivatives could be used to modify properties of the carrier without affecting the intended nature or practice of the invention. All such modifications are intended to be included within the scope of the claims.

The references cited within the text are incorporated herein by reference to the extent that they supplement, explain, provide a background for or teach methodology, techniques and/or compositions employed herein.

What is claimed is:

1. A method of preparing a radio-labelled liposome, comprising incubating the liposome with gamma-emitting radionuclide-labeled alkyleneamine oxime and an antioxidant, said incubating being for a period of time sufficient to form radio-labeled liposomes.

2. A method of preparing liposome-encapsulated radio-labelled protein, comprising incubating liposome-encapsulated protein with a gamma-emitting radionuclide-labeled alkyleneamine oxime and an antioxidant, said incubating being for a period of time sufficient to form labeled liposome-encapsulated protein.

3. The method of claim 1 or 2 wherein excess gamma-emitting radionuclide-labeled alkylene amine oxime is washed from the labeled liposomes or the liposome-encapsulated labeled protein.

4. The method of claim 1 or claim 2 wherein the antioxidant is a reductant.

5. The method of claim 1 or claim 2 wherein the antioxidant is glutathione or cysteine.

6. The method of claim 1 or claim 2 wherein the antioxidant is ascorbic acid.

7. The method of claim 1 or claim 2 wherein the antioxidant is reducing metal cation.

8. The method of claim 1 or claim 2 wherein the gamma-emitting radionuclide-labeled alkylene amine oxime comprises  $^{51}\text{Cr}$ ,  $^{59}\text{Fe}$ ,  $^{67}\text{Ga}$ ,  $^{86}\text{Rb}$ ,  $^{99m}\text{Tc}$ , and  $^{111}\text{In}$ .

9. The method of claim 1 or claim 2 wherein the gamma-emitting radionuclide-labeled alkyleneamine oxime is  $^{99m}\text{Tc}$ -hexamethylenepropylene amine oxime.

10. The method of claim 1 or claim 2 wherein the charge on the liposome is negative.

11. The method of claim 2 wherein the liposome-encapsulated protein is hemoglobin.

12. The method of claim 2 wherein the liposome-encapsulated protein is a  $^{99m}\text{Tc}$ -binding protein selected from the group consisting of albumin, transferring, myoglobin, myosin, insulin, globulin, casein, keratin, lectin, ferritin and elastin.

13. The method of claim 2 wherein the protein is at least partially denatured, said at least partially denatured protein binding a radionuclide label with greater affinity than the carrier.

14. The method of claim 2 wherein the protein is the  $\beta$ -chain of hemoglobin.

15. The method of claim 2 wherein the liposome-encapsulated labeled protein is liposome-encapsulated  $^{99m}\text{Tc}$ -hemoglobin.

16. A method of determining in vivo biodistribution, comprising

administering to an animal an amount of radio-labelled liposome prepared in accordance with claim 1 or claim 2, said amount being sufficient for detection by radiation detection and

determining in vivo biodistribution.

17. The method of claim 16 wherein the radio-labeled liposome comprises  $^{99m}\text{Tc}$ -hemoglobin.

18. The method of claim 16 wherein the radio-labeled liposome comprises  $^{99m}\text{Tc}$ -labeled liposome.

19. A method for labeling neutrophils, comprising the steps:

incubating neutrophils with liposome-encapsulated  $^{99m}\text{Tc}$ -hemoglobin or  $^{99m}\text{Tc}$ -labeled liposomes for a time sufficient to form  $^{99m}\text{Tc}$ -labeled neutrophils; and

separating the  $^{99m}\text{Tc}$ -labeled neutrophils.

20. A kit useful for preparing radiolabeled liposomes or liposome-encapsulated radiolabeled protein, comprising:

a transporter being compartmentalized to receive one or more container means in close confinement therein;

a first container means comprising an alkyleneamine oxide being capable of binding to a gamma-emitting radionuclide; and

a second container means comprising liposomes encapsulating a reducing agent or liposome-encapsulated protein and reducing agent.

21. The kit of claim 20 wherein the alkyleneamine oxime, the liposomes and the liposome-encapsulated protein are lyophilized.

22. The kit of claim 20 wherein the alkyleneamine oxime is hexamethylenepropylene amine oxime or propylene amine oxime.

23. The kit of claim 20 wherein the radionuclide is  $^{99m}\text{Tc}$ ,  $^{67}\text{Ga}$  or  $^{111}\text{In}$ .

24. The kit of claim 20 wherein the protein is hemoglobin, albumin, myoglobin, transferring or ferritin.

25. The kit of claim 20 wherein the reducing agent is glutathione or ascorbic acid.

26. A radionuclide-containing vesicle comprising  $^{99m}\text{Tc}$  bound to liposomes or liposome-encapsulated protein wherein a reducing agent is encapsulated with the liposomes or liposome-encapsulated protein.

27. The vesicle of claim 26 wherein the liposome-encapsulated protein is hemoglobin.

28. The vesicle of claim 26 wherein the reducing agent is glutathione or ascorbic acid.

29. A method of imaging bone marrow comprising the steps:

administering to an animal or human the radionuclide vesicle of claim 26 in an amount sufficient for detection by radiation detection means; and

determining distribution of the labelled vesicle after the vesicle has concentrated in the bone marrow.

30. The method of claim 29 wherein the imaging is determined about 20 hours after administration.

31. The method of claim 29 wherein the vesicles are liposomes about 0.1–0.2  $\mu$  in size.

\* \* \* \* \*

# $^{99m}\text{Tc}$ -PEG Liposomes for the Scintigraphic Detection of Infection and Inflammation: Clinical Evaluation

Els Th.M. Dams, Wim J.G. Oyen, Otto C. Boerman, Gert Storm, Peter Laverman, Peter J.M. Kok, Wilhelmina C.A.M. Buijs, Hans Bakker, Jos W.M. van der Meer, and Frans H.M. Corstens

*Departments of Nuclear Medicine, Internal Medicine, and Clinical Pharmaceutics, University Hospital Nijmegen, Nijmegen; and Institute for Pharmaceutical Science, Department of Pharmaceutics, Utrecht University, Utrecht, The Netherlands*

Polyethyleneglycol (PEG) liposomes have been shown to be excellent vehicles for scintigraphic imaging of infection and inflammation in various experimental models. In this article we report on a series of patients with possible infectious and inflammatory disease in whom the performance of  $^{99m}\text{Tc}$ -PEG liposomes was evaluated. The results of  $^{99m}\text{Tc}$ -PEG liposome scintigraphy were directly compared with those of  $^{111}\text{In}$ -immunoglobulin G (IgG) scintigraphy. **Methods:** Thirty-five patients (22 men, 13 women; mean age, 51 y; range, 20–76 y), suspected of having infectious or inflammatory disease, received 740 MBq  $^{99m}\text{Tc}$ -PEG liposomes intravenously. Imaging was performed at 4 and 24 h after injection. Patients received 75 MBq  $^{111}\text{In}$ -IgG 24 h after administration of the liposomes. The scintigraphic results were compared and verified by culture, biopsy, surgery, and follow-up of at least 6 mo. **Results:** Of the 16 proven infections and inflammations, 15 were detected by  $^{99m}\text{Tc}$ -PEG liposome scintigraphy: soft-tissue infection ( $n = 3$ ), septic arthritis ( $n = 3$ ), autoimmune polyarthritis ( $n = 2$ ), infected hip prosthesis ( $n = 1$ ), infected osteosynthesis ( $n = 1$ ), spondylodiscitis ( $n = 1$ ), infected aortic prosthesis ( $n = 1$ ), colitis ( $n = 1$ ), abdominal abscess ( $n = 1$ ), and pneumonia ( $n = 1$ ).  $^{99m}\text{Tc}$ -PEG liposome and  $^{111}\text{In}$ -IgG scintigraphy both missed 1 case of endocarditis. In addition, an  $^{111}\text{In}$ -IgG scan of a patient with mild soft-tissue infection was false-negative. Concordantly false-positive scans were recorded from 2 patients, both with uninfected pseudarthrosis and focal signs of sterile inflammation. During liposomal administration, 1 patient experienced flushing and chest tightness, which rapidly disappeared after lowering the infusion rate. No other adverse events were observed. **Conclusion:** This clinical evaluation of  $^{99m}\text{Tc}$ -PEG liposomes shows that focal infection and inflammation can be adequately imaged with this new agent. The performance of  $^{99m}\text{Tc}$ -PEG liposomes is at least as effective as that of  $^{111}\text{In}$ -IgG. With the simple and safe preparation and the physical and logistic advantages of a  $^{99m}\text{Tc}$  label,  $^{99m}\text{Tc}$ -PEG liposomes could be an attractive agent for infection or inflammation imaging.

**Key Words:**  $^{99m}\text{Tc}$ ; liposomes, polyethyleneglycol;  $^{111}\text{In}$ ; immunoglobulin G; imaging; infection; inflammation

J Nucl Med 2000; 41:622–630

Over the last decades several radiopharmaceuticals have been developed for the detection of infection and inflammation. Some have found their way into clinical practice and are routinely used for evaluation of infectious and inflammatory diseases (1–9). However, each of these agents has its limitations with regard to radiation dose, biodistribution, or preparation procedure, and thus the search for new and better agents for infection imaging continues. One of the newly developed and promising radiopharmaceuticals is radiolabeled liposomes. Liposomes are artificial phospholipid vesicles with an internal aqueous compartment. Since their discovery 30 y ago (10), they have been extensively investigated, mainly as potential carriers of therapeutic agents. The initial enthusiasm for liposomal carriers waned in the early 1980s because of the apparent limitations for radiopharmaceutical application (11). Rapid removal from the blood by cells of the mononuclear phagocyte system (MPS) compromised adequate targeting of non-MPS tissues. New insights in the recognition of liposomes by the MPS has led to the development of liposomes with long-circulating characteristics. Surface modification of liposomes with hydrophilic polymers such as polyethyleneglycol (PEG) resulted in decreased recognition by the MPS, and thus blood residence time was increased (12,13). As shown in both experimental and clinical studies, the enhanced circulatory half-life resulted in improved targeting potential of these PEG liposomes (14–17). Recently, we demonstrated the excellent performance of radiolabeled PEG liposomes in various animal models of infection and inflammation such as acute bacterial infection, colitis, arthritis, and chronic osteomyelitis (18–20). In addition, radiolabeled liposomes can be prepared relatively easily and can be labeled stably with  $^{99m}\text{Tc}$ . Furthermore, widespread experience with PEG-liposomal drug formulations has shown minimal or no toxic side effects (16,21–25).

The encouraging results of our experimental studies and the apparent safety of liposomal administration to humans prompted us to perform a clinical study to investigate the potential role of  $^{99m}\text{Tc}$ -labeled PEG liposomes in patients

Received Apr. 14, 1999; revision accepted Jul. 30, 1999.

For correspondence or reprints contact: Wim J.G. Oyen, MD, Department of Nuclear Medicine, University Hospital Nijmegen, P.O. Box 9101, 6500 HB Nijmegen, The Netherlands.

suspected of infectious or inflammatory disease. The results of  $^{99m}\text{Tc}$ -PEG liposome scintigraphy were directly compared with those of  $^{111}\text{In}$ -immunoglobulin G (IgG) scintigraphy, the standard procedure for infection imaging in our nuclear medicine department.

## MATERIALS AND METHODS

### Radiopharmaceuticals

**$^{99m}\text{Tc}$ -PEG-Hexamethyl Propyleneamine Oxime Liposomes.** Glutathione-containing PEG liposomes (hexamethyl propyleneamine [HMPAO] liposomes) were prepared as described previously (20). Each batch was checked for sterility and for absence of pyrogens. The mean size of the liposome preparations as determined by dynamic light scattering measurements was 80–100 nm, with a polydispersity index  $<0.1$ . Preformed glutathione-containing liposomes were labeled with  $^{99m}\text{Tc}$ , essentially as described previously (26). Briefly, the liposomes (70  $\mu\text{mol}$  phospholipid/mL) were incubated for 15 min at room temperature with freshly prepared  $^{99m}\text{Tc}$ -HMPAO (30 MBq/ $\mu\text{mol}$  phospholipid). Labeling efficiency was 60%–85%. Removal of unencapsulated  $^{99m}\text{Tc}$ -HMPAO was achieved by gel filtration on an extensively prerinsed PD-10 column (Pharmacia, Woerden, The Netherlands) with 5% glucose as the eluent. A dose of 35–40  $\mu\text{mol}$  PEG liposomes labeled with 740 MBq  $^{99m}\text{Tc}$  was administered intravenously.

**$^{111}\text{In}$ -IgG.** HIV and HBsAg-negative, human, nonspecific, polyclonal IgG (Gammagard; Baxter/Hyland, Lessines, Belgium) was conjugated with diethylenetriaminepentaacetic acid (DTPA) as described previously (7). Two or three DTPA-chelates were conjugated per IgG molecule. The conjugate was radiolabeled with  $^{111}\text{In}$  ( $^{111}\text{In}$ -chloride; Mallinckrodt, Inc., Petten, The Netherlands) by citrate transchelation. Labeling efficiency was always  $>95\%$ , as determined by instant thin-layer chromatography on silica gel strips (Gelman, Ann Arbor, MI) using 0.15 mol/L sodium citrate (pH 6.0) as the mobile phase. A dose of approximately 2 mg IgG labeled with 75 MBq  $^{111}\text{In}$  was injected intravenously.

**$^{111}\text{In}$ -Leukocytes.** First, total white blood cell (WBC) count and differentiation were determined from a blood sample from each patient. Then 50 mL blood were drawn by venapuncture in a syringe containing 10 mL acid citrate dextrose (ACD). Under strict sterile conditions, 6 mL 6% hydroxyethyl starch were added to 50 mL ACD-blood. The erythrocytes were allowed to sediment during 1 h. The supernatant was taken and centrifuged for 10 min at 150g. The cell pellet was washed with 5 mL 1% human serum albumin (HSA) solution in phosphate-buffered saline (PBS) pH 7.4 and centrifuged once more for 10 min at 150g. The cell pellet was resuspended in 1.5 mL 1% HSA solution in PBS.  $^{111}\text{In}$ -oxine ( $\sim 25$  MBq; Mallinckrodt) in 0.2 mol/L tris(hydroxymethyl)aminomethane (pH 8.0) was added to the cell suspension. Incubation at room temperature continued for 30 min. After centrifuging a third time for 10 min at 150g, the supernatant was discarded and the cell pellet was resuspended in 5 mL 1% HSA solution in PBS. Labeling efficiency, determined by measuring cell-associated and supernatant activity in a sample of the labeled WBC suspension, was always  $>95\%$ . A dose of 25 MBq  $^{111}\text{In}$ -WBC was injected intravenously.

### Patients

Thirty-five patients (22 men, 13 women; mean age, 51 y; range, 20–76 y) referred to the nuclear medicine department for imaging of infection or inflammation were studied prospectively. Informed

consent was obtained from each patient. Patients younger than 18 y and pregnant or lactating female patients were excluded from the study. The study protocol was approved by the ethical review board of the University Hospital Nijmegen, The Netherlands. Twenty-two patients were suspected of having infection or inflammation of the musculoskeletal system. Five patients had bacteremia and were referred either to localize the original focus or to investigate whether there was dissemination. Three patients had fever of unknown origin; 3 patients had possible abdominal pathologies; 1 patient was suspected of having endocarditis; and 1 patient was suspected of having an infected thrombus.

All 35 patients underwent  $^{99m}\text{Tc}$ -PEG liposome scintigraphy, and 34 also underwent  $^{111}\text{In}$ -DTPA-IgG scintigraphy. In 1 patient, who had a possibly infected aortic prosthesis,  $^{111}\text{In}$ -leukocytes scanning was performed as standard scintigraphic procedure. The scintigraphic results were verified by culture ( $n = 14$ ), biopsy ( $n = 1$ ), surgery ( $n = 11$ ), radiography ( $n = 17$ ), or clinical follow-up of at least 6 mo ( $n = 22$ ). Follow-up implied the absence of signs or symptoms of infection or inflammation in patients, confirming negative scintigraphic findings, or a favorable response to initiation of treatment, confirming positive scintigraphic results.

### Study Design

To avoid crossover of activity,  $^{99m}\text{Tc}$ -PEG liposome scintigraphy was performed 24 h before the standard scintigraphy with  $^{111}\text{In}$ -labeled agents (IgG or leukocytes).  $^{99m}\text{Tc}$ -PEG liposomes were administered as a bolus injection or slowly infused over a period of 10 min (3–4  $\mu\text{mol}/\text{min}$ ). Vital signs were recorded up to 1 h after injection. Blood samples were taken from all patients before and after  $^{99m}\text{Tc}$ -PEG liposome scintigraphy for hematologic and biochemical evaluation. In 7 patients blood samples were taken for measurement of the blood clearance of  $^{99m}\text{Tc}$ -PEG liposomes. In addition, urine was collected during a 24-h period to estimate the excretion of the  $^{99m}\text{Tc}$  label.

### Imaging Protocol and Image Interpretation

Scintigraphic images were obtained with a Siemens Orbiter connected to a Scintiview image processor or a MultiSpect 2  $\gamma$  camera connected to an ICON computer system (Siemens Inc., Hoffman Estates, IL). All images were collected in digital format in a  $256 \times 256$  or a  $256 \times 1024$  matrix. Whole-body scans of  $^{99m}\text{Tc}$ -liposomes were recorded at 4 h (scan speed, 15 cm/min) and 24 h after injection (scan speed, 6 cm/min). Additional SPECT images were acquired if abdominal abnormalities were suspected. If indicated, spot views of  $^{99m}\text{Tc}$ -PEG liposomes were acquired at 4 and 24 h after injection for a preset time of 5 and 15 min, respectively, using a low-energy, high-resolution, parallel-hole collimator (140-keV photopeak, 15% symmetric window).

$^{111}\text{In}$ -labeled IgG or leukocytes were administered 24 h after the administration of  $^{99m}\text{Tc}$ -PEG liposomes, and spot views were acquired at 4, 24, and 48 h after injection, with a preset time of 5, 7.5, and 10 min, respectively, using a medium-energy, parallel-hole collimator (15% symmetric window for both the 173- and the 247-keV energy peaks). We have previously shown that in such settings the scatter of  $^{99m}\text{Tc}$  in the  $^{111}\text{In}$  images at 4 h after injection is  $<1\%$  (27).

Images were read by 2 nuclear medicine physicians who were unaware of the results of the verification procedures. Both  $^{99m}\text{Tc}$ -PEG liposome and  $^{111}\text{In}$ -IgG scans were considered positive for inflammation or infection if focal and, with time, increasing accumulation of tracer was observed.

## Blodistribution and Dosimetry

To calculate the uptake of  $^{99m}\text{Tc}$ -PEG liposomes in various organs, 9 patients underwent additional imaging, including whole-body images at 15 min after injection (scan speed, 15 cm/min) and SPECT images of the abdominal organs. Regions of interest (ROIs) were drawn around the whole body, lungs, liver, spleen, kidneys, and testes. Estimates of absolute activity uptake in these organs were made by calculating the geometric mean of activity in an organ ROI, corrected for radioactive decay. Organ radioactivity as percentage injected dose (%ID) was estimated by using the whole-body ROI of the first scan as 100% of the administered dose. The absorbed doses to the organs and the effective dose were calculated using the MIRD scheme.

Blood and urine samples were collected and the content of radioactivity was determined. To correct for physical decay and to calculate activity in blood and urine as a fraction of the injected dose, injection standards were counted simultaneously. Whole-blood data were analyzed by nonlinear least-squares fit using a biexponential model.

## RESULTS

Thirty-five patients with 49 possible infectious and inflammatory foci were investigated. The individual clinical characteristics and the results of the scintigraphic and verification procedures are summarized in Table 1. Figure 1 shows a representative whole-body image 24 h after injection of  $^{99m}\text{Tc}$ -PEG liposomes. This image clearly illustrates the physiologic uptake of the agent in the cardiac blood pool, larger blood vessels, liver and spleen, and, to a lesser extent, the kidneys. Uptake in lung, bone, and gastrointestinal tract was low. The prolonged circulation time of PEG liposomes is apparent from the blood clearance curve (Fig. 2) showing a  $t_{1/2\alpha}$  of  $0.31 \pm 0.09$  h and a  $t_{1/2\beta}$  of  $58.1 \pm 17.0$  h. The mean whole-body retention at 4 and 24 h after injection was  $87.0 \pm 4.8$  %ID and  $79.8 \pm 10.9$  %ID, respectively. The radioactivity was excreted mainly through the kidneys ( $19.3 \pm 6.3$  %ID in the urine in the first 24 h). The mean organ uptakes of labeled liposomes at various time points are shown in Table 2. After initial uptake of activity, no further accumulation or release of activity from the source organs was found. The mean absorbed doses to the organs are presented in Table 3. The mean effective dose was  $7.6 \pm 0.5$   $\mu\text{Sv}/\text{MBq}$ . For a typical administered activity of 740 MBq  $^{99m}\text{Tc}$ -PEG liposomes, the dose to the red marrow was 3.0 mGy, the dose to the testes was 9.6 mGy, and the effective dose was 5.6 mSv.

During injection of the labeled liposomes, 1 patient, with a history of hyperventilation, experienced mild flushing and tightness of the chest, which subsided when the injection was temporarily stopped. On the scintigram acquired 4 h later, increased uptake in liver and spleen and decreased activity in the heart region were noted, indicating enhanced blood clearance of the agent in this patient. None of the other patients experienced any side effects, nor were there any significant changes in hematologic or biochemical values.

Sixteen of the 35 investigated patients had proven infections or inflammations (Table 1), with a total of 28 foci.

$^{99m}\text{Tc}$ -liposome scintigraphy correctly identified 27 of these foci in 15 patients.  $^{111}\text{In}$ -IgG scintigraphy, performed in 15 of the 16 positive patients, visualized 25 of 27 foci in 13 patients. The sixteenth patient underwent  $^{111}\text{In}$ -leukocytes scintigraphy as the second procedure, which correctly identified the infectious lesion. Nine patients, including 1 patient with a spondylodiscitis, had infections of the locomotor system; 2 patients had noninfectious polyarthritis; 1 had an infected aortic prosthesis; 1 had a pneumonia; 1 patient had endocarditis; 1 had colitis; and 1 patient had an abdominal abscess. Examples of abnormal  $^{99m}\text{Tc}$ -liposome and  $^{111}\text{In}$ -IgG scintigrams are shown in Figures 3–5.

The results of  $^{99m}\text{Tc}$ -liposome and  $^{111}\text{In}$ -IgG scintigraphy were discordant in 1 patient. This patient, a 40-y-old man, was referred to our department to exclude a diagnosis of osteomyelitis because of swelling and redness at the level of an old tibial fracture. Increased focal uptake was seen with the liposomes but not with  $^{111}\text{In}$ -IgG (Fig. 3). Although no cultures were acquired in this patient, the findings on physical examination and the rapid improvement with antibiotic treatment were consistent with soft-tissue infection, and the patient was classified as true-positive for  $^{99m}\text{Tc}$ -liposome scintigraphy and false-negative for  $^{111}\text{In}$ -IgG. In 2 other patients, both scans were classified as true-positive, but the extent and the severity of the disease were more clearly visualized on the  $^{99m}\text{Tc}$ -liposome scintigram (Fig. 4).

The results of  $^{99m}\text{Tc}$ -liposome and  $^{111}\text{In}$ -leukocyte scintigraphy in patient 16 were classified as concordantly true-positive. This 75-y-old man was referred because of persistent fever and possibly infected aortic graft. Both scans showed focal uptake of the radiolabel around the prosthesis, consistent with findings on MRI. Surgery was not performed because of severe cardiac disease. Although cultures remained negative, clinical improvement on antibiotic treatment and the absence of other apparent foci were found to be consistent with a diagnosis of an infected aortic prosthesis.

A concordantly false-negative result of  $^{99m}\text{Tc}$ -liposomes and  $^{111}\text{In}$ -IgG was obtained in a 43-y-old patient with a 3-wk history of fever and back pain. He was suspected of having endocarditis and was referred for infection scanning to exclude spondylodiscitis. Both scans gave negative results in accordance with radiographic findings. Subsequent blood cultures grew *S. sanguis*, and the patient was started on antibiotic treatment. Initially, echocardiography gave negative results, but a repeated study 1 mo later showed thickening of the mitral valve and regurgitation, consistent with a diagnosis of endocarditis. Although this had not been the reason for referral, and the clinician had been aware of the limited usefulness of the standard scintigraphic procedure in visualizing endocarditis, both scans were classified as false-negative.

False-positive scans were recorded in 2 patients with pseudoarthroses, both with  $^{99m}\text{Tc}$ -liposome and  $^{111}\text{In}$ -IgG scintigraphy. In both cases, focal signs of inflammation were noted at surgery, but cultures remained negative.

**TABLE 1**  
Clinical Characteristics, Results of Scintigraphy, and Verification Procedures

Patient no.	Sex	Age (y)	Duration	Suspected focus	Scintigraphy		Verification	
					<sup>99m</sup> Tc-liposome	<sup>111</sup> In-IgG	Procedure	Result
1	M	40	2 wk	Tibia	+	—	Bo, FU	Soft-tissue infection
2	M	20	1 mo	Colon	+	+	E, B	Colitis
3	M	62	4 wk	Knee	+	+	Bo, FU	Bursitis
4	F	46	3 d	Shoulder, elbow, wrist, ankles, knee	+	+	C, FU	Autoimmune polyarthritis
5	M	76	2 wk	Treated SP bacteremia; hip	+	+	R, C, FU	SP septic arthritis
6	M	42	4 wk	Hip	+	+	S	SA septic arthritis
7	M	58	2 mo	Shoulders, hips, wrists, small hand joints	+	+	C, FU	Rheumatoid arthritis
8	M	24	1 wk	Abdomen	+	+	S	BF abscess
9	F	75	2 wk	Spine	+	+	S	SA spondylodiscitis
10	M	29	4 d	SP bacteremia; lung, shoulder	+	+	R, C, FU	SP pneumonia No arthritis
11	M	65	1 wk	SP bacteremia; hip	+	+	C, FU	SP septic arthritis
12	M	63	3 mo	Total hip prosthesis	+	+	R, FU	Bursitis
13	F	66	2 mo	Total hip prosthesis	+	+	R, C, FU	SA-infected prosthesis
14	M	21	1 mo	Tibia	+	+	S	SA-infected osteosynthesis
15	M	43	4 wk	Endocarditis; spine	—	—	R, C	SS endocarditis No spondylodiscitis
16	M	75	2 mo	Fever of unknown origin	+	+ ( <sup>111</sup> In-WBC)	R, FU	Infected aortic prosthesis
17	F	72	4 mo	Tibia	+	+	S	Pseudoarthrosis
18	F	28	1 y	Ankle	+	+	S	Pseudoarthrosis
19	M	44	18 mo	Girdlestone	—	—	S	No infection
20	F	58	1 y	Total knee prosthesis	—	—	R, FU	No infection
21	M	45	3 wk	Treated SH bacteremia; persisting fever	—	—	R, C, FU	No cause identified Fever subsided
22	M	55	1 y	Girdlestone	—	—	C, FU	No infection
23	F	71	18 mo	Total knee prosthesis	—	—	S	Loosening prosthesis
24	M	21	14 mo	Ankle	—	—	S	Noninfected osteosynthesis
25	M	58	1 y	Total hip prosthesis	—	—	S	Loosening prosthesis
26	F	71	18 mo	Total hip prosthesis	—	—	S	Pseudoarthrosis
27	F	54	1 y	Spine	—	—	R, C, FU	Noninfected osteosynthesis
28	F	65	2 y	Total knee prosthesis	—	—	R, FU	No infection
29	M	42	1 y	Total knee prosthesis	—	—	R, C, FU	Radicular syndrome
30	F	35	5 y	Fever of unknown origin	—	—	R, C, FU	Factitious fever
31	M	56	4 y	Fever of unknown origin	—	—	R, C, FU	No cause identified
32	M	29	1 wk	Colon	—	—	R, C, FU	Resolved diverticulitis
33	F	63	2 wk	Treated SE bacteremia; total knee prosthesis	—	—	R, FU	No infection
34	M	24	1 wk	Iliacal vessel	—	—	R, FU	No infection
35	M	75	2 mo	Crista	—	—	R, FU	No infection

Bo = bone scan; FU = clinical follow-up of at least 6 mo; E = endoscopy; B = biopsy; C = bacterial culture; SP = *Streptococcus pneumoniae*; R = radiologic procedures; S = surgery; SA = *Staphylococcus aureus*; BF = *Bacteroides fragilis*; SS = *Streptococcus sanguis*; SH = *Streptococcus hemolyticus*; SE = *Staphylococcus epidermis*.

The 17 patients with true-negative <sup>99m</sup>Tc-liposome scans included 2 patients with bacteremia. Patient 21, a 45-y-old man, had been admitted with a *S. hemolyticus* sepsis and was referred because of persisting subfebrile temperature despite adequate antibiotic treatment. The negative scintigraphic findings were classified as true-negative because cultures remained sterile, whereas the temperature normalized spontaneously. Patient 33 was a 63-y-old woman who had been treated for *S. epidermidis* bacteremia. She had temporarily complained of a painful knee and was referred to exclude bacterial infection of her knee prosthesis. The negative

scintigraphic results were in accordance with the clinical follow-up and were therefore considered to be true-negative. Two patients with fever of unknown origin were also classified as true-negative. Patient 30, a 35-y-old woman, appeared to have factitious fever. In patient 31, the fever subsided, and the verification procedures remained negative.

The sensitivity and specificity of <sup>99m</sup>Tc-liposome scintigraphy in this group of patients were 94% and 89%, respectively. For <sup>111</sup>In-IgG, these figures were 87% and 89%, respectively.

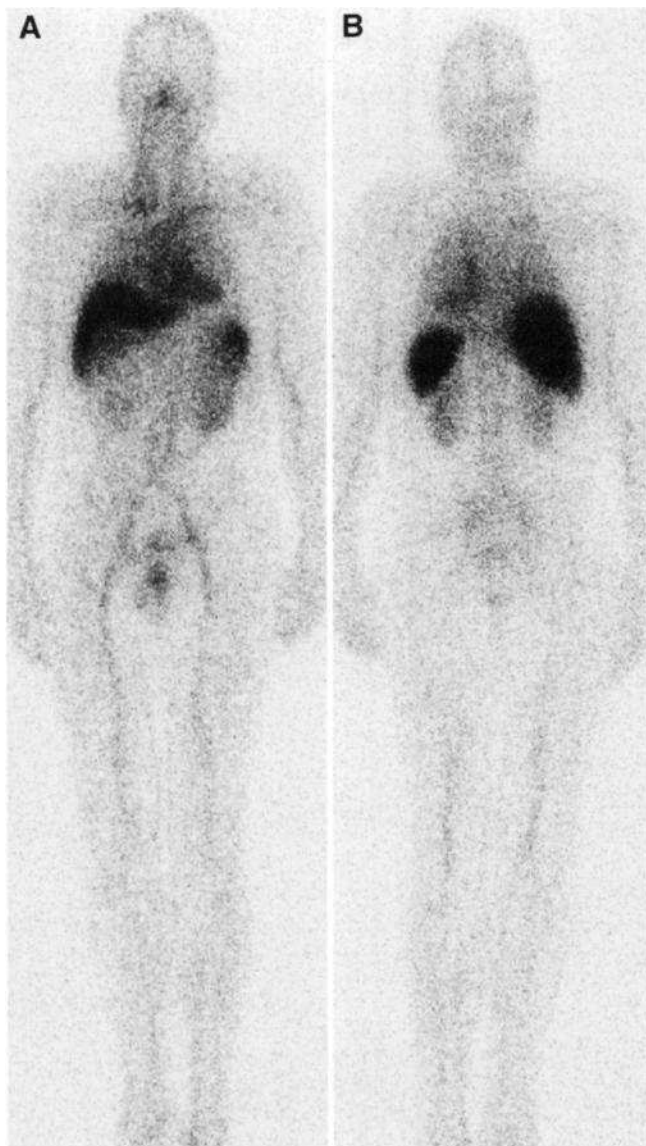


**FIGURE 1.** Anterior (A) and posterior (B) whole-body  $^{99m}\text{Tc}$ -PEG liposome scintigrams show normal distribution of radiolabel 24 h after injection.

## DISCUSSION

In recent years, the potential of PEG liposomes to target pathologic lesions has been exploited successfully in the field of drug targeting. As carriers of therapeutic agents, they have been shown to reduce drug-related toxicity and to increase the therapeutic efficacy of a given drug (14–17,28). These favorable results have inspired research into the use of radiolabeled PEG liposomes for scintigraphic imaging of infection and inflammation (18–20). This article reports on a clinical study with radiolabeled PEG liposomes for evaluation of patients with suspected infectious and inflammatory diseases. In this group of patients with predominantly musculoskeletal pathologies,  $^{99m}\text{Tc}$ -PEG liposome scintigraphy showed high sensitivity and specificity. All infectious and inflammatory foci were detected, with only 1 case of endocarditis missed. The visualization of musculoskeletal

and abdominal pathology was better than with  $^{111}\text{In}$ -IgG scintigraphy. Although  $^{111}\text{In}$ -IgG is not considered the gold standard in nuclear medicine for infection imaging, its excellent performance in delineating locomotor infections has been well established (29). The more accurate delineation of abdominal inflammation with radiolabeled PEG liposomes compared with radiolabeled IgG is in agreement with our previous findings in experimental colitis (30,31). Still, our findings are remarkable, because both liposomes and IgG are thought to accumulate in inflammatory areas according to the same nonspecific mechanism and have similar slow blood clearance (32). Although the more optimal physical properties of the  $^{99m}\text{Tc}$  label could explain the observed differences, the concordance of  $^{99m}\text{Tc}$ -hydrazino nicotinamide (HYNIC) IgG and  $^{111}\text{In}$ -IgG in a similar clinical study (27) suggests an additional cause. According to Peters and Jamar (33), unidirectional transport of macromolecules from plasma to interstitial fluid becomes more predominant with increasing molecular size, because in these situations convective transport rather than diffusion will prevail. Thus, reverse diffusion of the smaller IgG from the interstitial fluid to the bloodstream could result in lower extravascular concentration.

The nonspecific uptake mechanism of both agents could lead to false-positive results, as illustrated in this study. Uptake of  $^{111}\text{In}$ -IgG in pseudoarthrosis has been described previously and is attributed to noninfectious inflammation as a result of irritation from motion at the unstable sites (29).

The nonspecific nature of labeled liposomes—in contrast with the current trend in nuclear medicine toward specific receptor binding—is not necessarily disadvantageous. First, uptake at sites of sterile inflammation could very well answer the clinician's question, as illustrated by the patients with polyarthritis and colitis. Second, knowledge of the clinical data and experience with patterns of nonpathologic uptake will help to correctly interpret the scintigraphic results and thus increase specificity. For example, the visualization of the synovial lining in patient 7 could easily be distinguished from the diffuse, intense uptake seen in septic arthritis.

One of the major diagnostic problems in the imaging of infections is the adequate assessment of chronic osteomyelitis. Whether labeled liposomes could be of value remains to be assessed, because chronic osteomyelitis was not evaluated in this study. Still, the adequate visualization of other types of chronic infections and the promising performance of the agent in experimental chronic osteomyelitis (19) suggest that  $^{99m}\text{Tc}$ -PEG liposomes could be a useful diagnostic tool.

Although the infectious and inflammatory lesions were generally positive at 4 h after injection, visualization was improved at 24 h after injection as a result of increasing focal uptake and decreasing background activity. However, physiologic uptake in liver and spleen could mask abscesses in the upper abdomen. The relatively high background activity of labeled liposomes, resulting from the prolonged

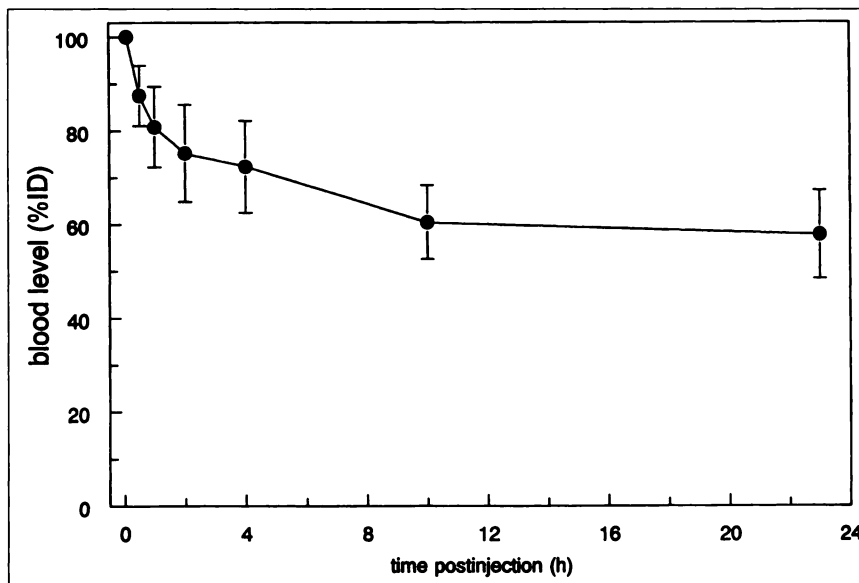


**FIGURE 2.** Blood clearance of <sup>99m</sup>Tc-PEG liposomes in 7 patients. Blood-pool activity measured 5 min after injection was set at 100%. Error bars represent SD.

blood residence time, might hamper adequate delineation of infections in well-perfused tissues, as was apparent in the patient with endocarditis. One of the options to decrease blood-pool activity of liposomes without compromising focal accumulation could be the application of the biotin-avidin system, as we have shown recently (34). Whether this approach will lead to improved visualization of infections such as endocarditis and vascular graft infections awaits additional studies.

In this study, the liposomes were labeled according to the method described by Phillips et al. (26). A disadvantage of this method is the relatively complex technique for preparation, requiring postlabeling purification because of the relatively low labeling efficiency (60%–85%). Recently, we described a new method to label liposomes with <sup>99m</sup>Tc-pertechnetate using HYNIC conjugated to distearoylphosphatidyl-ethanolamine (35). This HYNIC-based method provides <sup>99m</sup>Tc-labeled liposomes with high labeling efficiency (>95%) and improved in vitro and in vivo characteristics. Because HYNIC-derivatized PEG liposomes can be made available as a kit for instant <sup>99m</sup>Tc labeling with pertechnetate, an additional advantage is the reduction of costs,

because extensive laboratory handling for postlabeling purification is no longer necessary and HMPAO kits are no longer necessary as an intermediate for <sup>99m</sup>Tc labeling of the PEG liposomes (35). Given the advantages of this new labeling method, further clinical studies will be conducted with <sup>99m</sup>Tc-HYNIC PEG liposomes.

The acute reaction to liposomal administration observed in 1 patient in this study has been reported in clinical trials with PEG-liposomal doxorubicin (15,24). However, we found its occurrence rather surprising because much lower doses were used in our protocol (~0.5 μmol phospholipid/kg body weight) compared with the dose for therapeutic purposes (~10 μmol phospholipid/kg body weight). It has been suggested that activation of complement with subsequent release of vasoactive mediators may have caused the reported side effects (36). In this context, enhanced opsonization of the administered liposomes is likely to occur concurrently and could thus explain the rapid blood clearance of the agent in our patient. Because the acute reaction is thought to be provoked by a fast rate of infusion in susceptible patients (24), we converted the administration of

**TABLE 2**  
Organ Uptake of <sup>99m</sup>Tc-PEG Liposomes (%ID)

Site	Time after injection		
	15 min	4 h	24 h
Liver*	10.5 ± 3.6	9.8 ± 3.4	10.1 ± 3.8
Spleen*	3.4 ± 1.6	4.6 ± 3.0	4.0 ± 2.2
Kidneys*	3.0 ± 1.8	2.8 ± 1.3	3.2 ± 1.7
Testes†	0.6 ± 0.1	0.5 ± 0.1	0.4 ± 0.1
Whole body*	100	87.0 ± 4.8	79.8 ± 10.9

\*Mean ± SD for 9 patients.  
†Mean ± SD for 5 male patients.

**TABLE 3**  
Absorbed Doses in Organs (μGy/MBq)

Site	<sup>99m</sup> Tc-PEG liposomes
Liver*	11 ± 3
Spleen*	29 ± 14
Kidneys*	15 ± 5
Bone marrow*	4 ± 1
Testes†	13 ± 3
Urinary bladder wall*	16 ± 4

\*Mean ± SD for 9 patients.  
†Mean ± SD for 5 male patients.



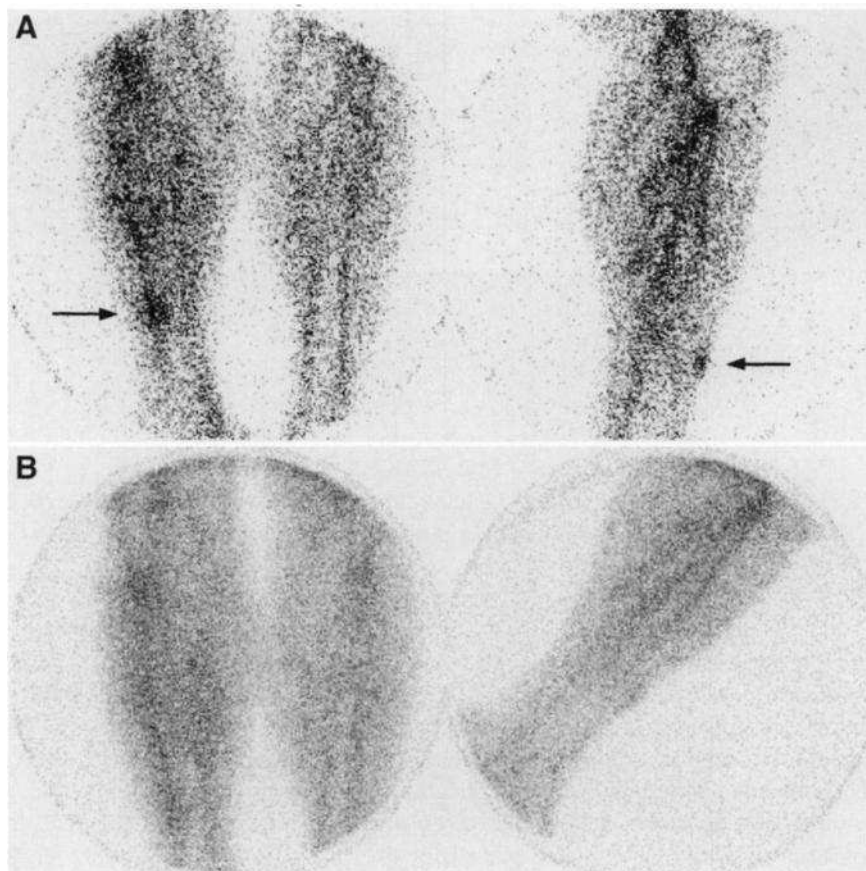


**FIGURE 3.** True-positive  $^{99m}\text{Tc}$ -PEG liposome scintigram and false-negative  $^{111}\text{In}$ -IgG scintigram in patient 1 (40-y-old man) with painful swelling and redness at level of old tibial fracture. (A)  $^{99m}\text{Tc}$ -PEG liposome scintigram, lateral view, 24 h after injection. Increased uptake in lower leg consistent with soft-tissue infection (arrow). (B)  $^{111}\text{In}$ -IgG scintigram, 24 h after injection. Absence of abnormal accumulation in lower leg.

the radiopharmaceutical from a bolus injection to a slow infusion. Furthermore, the new HYNIC-labeling method allows the preparation of liposomes with a higher specific activity and thus the administration of a lower lipid dose.

Comparing the biodistribution data for  $^{99m}\text{Tc}$ -PEG liposomes with those reported for  $^{111}\text{In}$ -IgG (37), the uptakes of activity in the liver and kidney were relatively low (9.9% versus 19.2% and 3.2% versus 7.2%, respectively). The relatively low liver uptake illustrates the MPS-evading properties of the PEG liposomes. The uptake in the spleen was somewhat higher, and the testicular uptake was similar

to that of  $^{111}\text{In}$ -IgG (37). The effective dose for  $^{99m}\text{Tc}$ -PEG liposomes was 7.6  $\mu\text{Sv}/\text{MBq}$ . This is in the same range as that of other  $^{99m}\text{Tc}$ -labeled agents used for infection imaging, such as  $^{99m}\text{Tc}$ -labeled WBCs (11  $\mu\text{Sv}/\text{MBq}$ ) and  $^{99m}\text{Tc}$ -labeled diphosphonate (6.0  $\mu\text{Sv}/\text{MBq}$ ) (38). Therefore, from a radiation safety point of view, this radiopharmaceutical can be administered safely.

## CONCLUSION

This clinical evaluation of  $^{99m}\text{Tc}$ -PEG liposomes indicates that this new agent offers a safe and effective scintigraphic

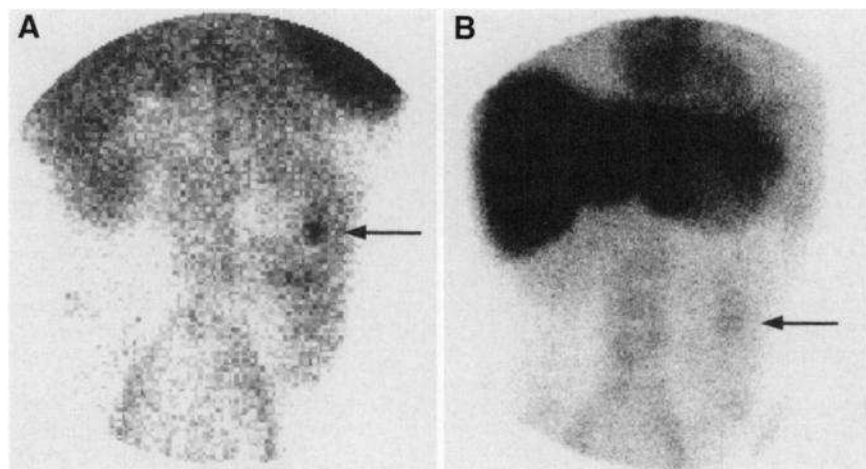


**FIGURE 4.** Abdominal planar views, 24 h after injection of  $^{99m}\text{Tc}$ -PEG liposomes (A) and  $^{111}\text{In}$ -IgG (B) in patient 2 (20-y-old man) with Crohn's disease. Although both scans show diffuse accumulation in distal colon, liposomes scintigram more accurately depicts extent and severity of colitis. Arrow points to hot spot midway in colon, consistent with focal ulceration as confirmed by endoscopic and histologic examination.



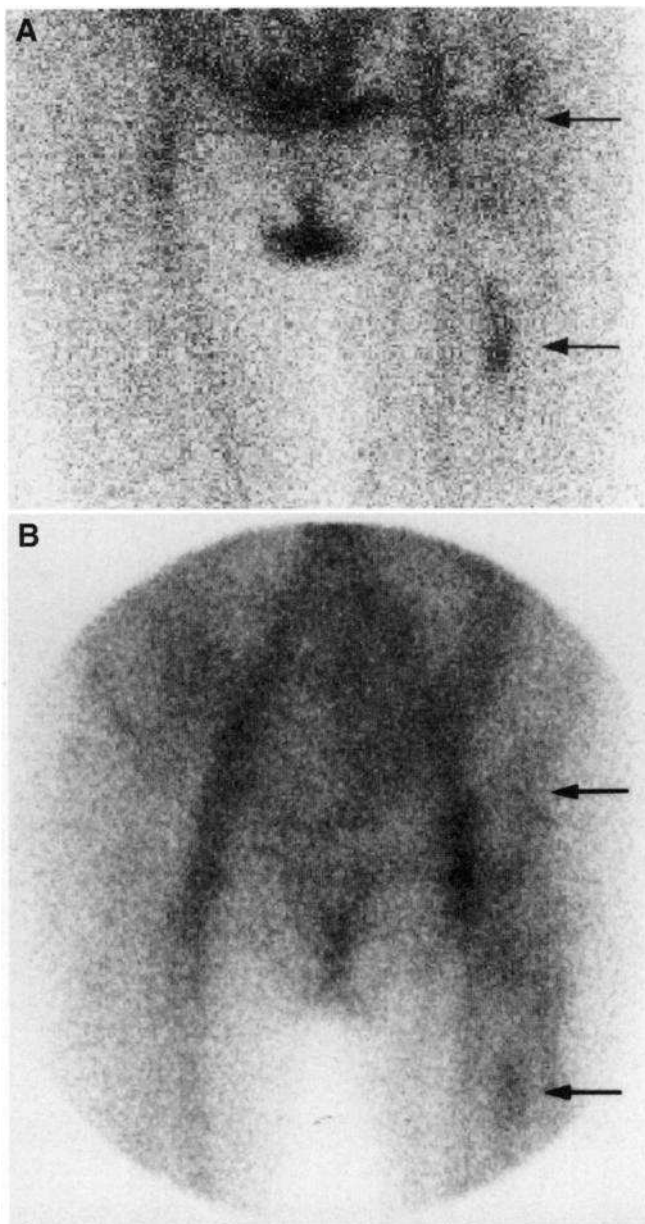


**FIGURE 5.** Concordantly positive  $^{99m}\text{Tc}$ -PEG liposome scintigram (A) and  $^{111}\text{In}$ -IgG scintigram (B) in patient 13 (66-y-old woman) with fever, elevated erythrocyte sedimentation rate, and painful left hip prosthesis. Both scans show increased uptake around prosthesis and femoral shaft (arrows). Cultures revealed growth of *S. aureus*. Patient responded favorably to initiation of antibiotic treatment.

method to target focal infection and inflammation. Its performance is at least as good as that of  $^{111}\text{In}$ -IgG scintigraphy. The sensitivity and specificity of  $^{99m}\text{Tc}$ -PEG liposomes for imaging infection or inflammation (or both) appeared to be in the range needed for routine clinical practice. The agent is easily prepared and has the physical and logistic advantages of a  $^{99m}\text{Tc}$  label. These studies show that  $^{99m}\text{Tc}$ -PEG liposomes is a promising radiopharmaceutical for the scintigraphic evaluation of infection and inflammation.

## ACKNOWLEDGMENTS

The guidance of Prof. Dr. J.H. Beijnen (Slotervaart Ziekenhuis, Amsterdam, The Netherlands) in the preparation of the liposomes for clinical use is gratefully acknowledged. The authors also thank Mr. E. Koenders for his assistance in the radiolabeling of the liposomes. The study was supported by grant NGN 55.3665 from the Technology Foundation (Technologiestichting STW), The Netherlands.

## REFERENCES

1. Lavender JP, Lowe J, Barker JR, Burn JJ, Chaudhri MA. Gallium-67 citrate scanning in neoplastic and inflammatory lesions. *Br J Radiol.* 1971;44:361-366.
2. Palestro CJ. The current role of gallium imaging in infection. *Semin Nucl Med.* 1994;24:128-141.
3. Thakur ML, Lavender JP, Arnot RN, Silvester DJ, Segal AW. Indium-111-labeled autologous leukocytes in man. *J Nucl Med.* 1977;18:1012-1021.
4. Datz FL. Indium-111-labeled leukocytes for the detection of infection: current status. *Semin Nucl Med.* 1994;24:92-109.
5. Peters AM, Danpure HJ, Osman S, et al. Clinical experience with  $^{99m}\text{Tc}$ -hexamethylpropylene-amine oxime for labelling leucocytes and imaging inflammation. *Lancet.* 1986;2:946-949.
6. Rubin RH, Fischman AJ, Callahan RJ, et al.  $^{111}\text{In}$ -labeled nonspecific immunoglobulin scanning in the detection of focal infection. *N Engl J Med.* 1989;321:935-940.
7. Oyen WJG, Claessens RAMJ, van Horn JR, van der Meer JWM, Corstens FHM. Scintigraphic detection of bone and joint infections with indium-111 labeled nonspecific polyclonal human immunoglobulin G. *J Nucl Med.* 1990;31:403-412.
8. Arndt JW, van der Sluis-Veer A, Blok D, et al. A prospective comparison of  $^{99m}\text{Tc}$ -labeled polyclonal human immunoglobulin and  $^{111}\text{In}$  granulocytes for localization of inflammatory bowel disease. *Acta Radiol.* 1992;33:140-144.
9. Becker W, Goldenberg DM, Wolf F. The use of monoclonal antibodies and antibody fragments in the imaging of infectious lesions. *Semin Nucl Med.* 1994;24:142-153.
10. Bangham AD, Horne RW. Negative staining of phospholipids and their structural modification by surface-active agents as observed in the electron microscope. *J Mol Biol.* 1964;8:660-668.
11. Morgan JR, Williams LA, Howard CB. Technetium-labelled liposomes imaging for deep-seated infections. *Br J Radiol.* 1985;85:35-39.
12. Woodle MC, Lasic DD. Sterically stabilized liposomes. *Biochim Biophys Acta.* 1992;1113:171-199.
13. Allen TM, Hansen C, Martin F, Redemann C, Yau Young A. Liposomes containing synthetic lipid derivatives of poly(ethylene glycol) show prolonged circulation half-lives in vivo. *Biochim Biophys Acta.* 1991;1066:29-36.
14. Huang SK, Mayhew E, Gilani S, Lasic DD, Martin FJ, Papahadjopoulos D. Pharmacokinetics and therapeutics of sterically stabilized liposomes in mice bearing C-26 colon carcinoma. *Cancer Res.* 1992;52:6774-6781.
15. Gabizon AA. Selective tumor localization and improved therapeutic index of anthracyclines encapsulated in long-circulating liposomes. *Cancer Res.* 1992;52:891-896.
16. Gabizon A, Catane R, Uziely B, et al. Prolonged circulation time and enhanced accumulation in malignant exudates of doxorubicin encapsulated in polyethylene-glycol coated liposomes. *Cancer Res.* 1994;54:987-992.
17. Bakker-Woudenberg IA, Lokker AF, ten Kate MT, Mouton JW, Woodle MC, Storm G. Liposomes with prolonged blood circulation and selective localization in Klebsiella pneumoniae-infected lung tissue. *J Infect Dis.* 1993;168:164-171.
18. Boerman OC, Storm G, Oyen WJG, et al. Sterically stabilized liposomes labeled with indium-111 for imaging focal infection in rats. *J Nucl Med.* 1995;36:1639-1644.
19. Laverman P, Boerman OC, Oyen WJG, Dams ETM, Storm G, Corstens FHM. Liposomes for scintigraphic detection of infection and inflammation. *Adv Drug Deliv Rev.* 1999;37:225-235.
20. Oyen WJG, Boerman OC, Storm G, et al. Detecting infection and inflammation with technetium-99m-labeled stealth liposomes. *J Nucl Med.* 1996;37:1392-1397.
21. Muggia FM, Hainsworth JD, Jeffers S, et al. Phase II study of liposomal doxorubicin in refractory ovarian cancer: antitumor activity and toxicity modification by liposomal encapsulation. *J Clin Oncol.* 1997;15:987-993.
22. Goebel FD, Goldstein D, Goos M, Jablonowski H, Stewart JS. Efficacy and safety of stealth liposomal doxorubicin in AIDS-related Kaposi's sarcoma: the International SL-DOX Study Group. *Br J Cancer.* 1996;73:989-994.
23. Northfelt DW, Dezube BJ, Thommes JA, et al. Efficacy of pegylated-liposomal doxorubicin in the treatment of AIDS-related Kaposi's sarcoma after failure of standard chemotherapy. *J Clin Oncol.* 1997;15:653-659.

24. Uziely B, Jeffers S, Isacson R, et al. Liposomal doxorubicin: antitumor activity and unique toxicities during two complementary phase I studies. *J Clin Oncol.* 1995;13:1777-1785.
25. Harrison M, Tomlinson D, Stewart S. Liposomal-entrapped doxorubicin: an active agent in AIDS-related Kaposi's sarcoma. *J Clin Oncol.* 1995;13:914-920.
26. Phillips WT, Rudolph AS, Goins B, Timmons JH, Klipper R, Blumhardt R. A simple method for producing a technetium-99m-labeled liposome which is stable in vivo. *Int J Rad Appl Instrum B.* 1992;19:539-547.
27. Dams ETM, Oyen WJG, Boerman OC, et al. Technetium-99m labeled to human immunoglobulin G through the nicotinyl hydrazine derivative: a clinical study. *J Nucl Med.* 1998;39:119-124.
28. Van Etten EW, Snijders SV, van Vianen W, Bakker-Woudenberg IA. Superior efficacy of liposomal amphotericin B with prolonged circulation in blood in the treatment of severe candidiasis in leukopenic mice. *Antimicrob Agents Chemother.* 1998;42:2431-2433.
29. Nijhof MW, Oyen WJG, van Kampen A, Claessens RAMJ, van der Meer JWM, Corstens FHM. Evaluation of infections of the locomotor system with In-111-labeled human IgG scintigraphy. *J Nucl Med.* 1997;38:1300-1305.
30. Oyen WJG, Boerman OC, Dams ETM, et al. Scintigraphic evaluation of experimental colitis in rabbits. *J Nucl Med.* 1997;38:1596-1600.
31. Dams ETM, Oyen WJG, Boerman OC, et al. Tc-99m-labeled PEG-liposomes to image experimental colitis in rabbits: comparison with Tc-99m-HMPAO-granulocytes and Tc-99m-HYNIC-IgG. *J Nucl Med.* 1998;39:2172-2178.
32. Oyen WJG, Boerman OC, van der Laken CJ, Claessens RAMJ, van der Meer JWM, Corstens FHM. The uptake mechanisms of inflammation and infection localizing agents. *Eur J Nucl Med.* 1996;23:459-465.
33. Peters AM, Jamar F. The importance of endothelium and interstitial fluid in nuclear medicine. *Eur J Nucl Med.* 1998;25:801-815.
34. Laverman P, Oyen WJG, Storm G, et al. Avidin-induced clearance of Tc-99m-biotin-PEG-liposomes to image focal infections [abstract]. *Eur J Nucl Med.* 1998;25:886.
35. Laverman P, Dams ETM, Oyen WJG, et al. A novel method to label liposomes with Tc-99m via the hydrazino nicotinyl derivative. *J Nucl Med.* 1999;40:192-197.
36. Szebeni J. The interaction of liposomes with the complement system. *Crit Rev Ther Drug Carrier Syst.* 1998;15:57-88.
37. Buijs WCAM, Oyen WJG, Dams ETM, et al. Dynamic distribution and dosimetric evaluation of human nonspecific immunoglobulin G labeled with In-111 or Tc-99m. *Nucl Med Commun.* 1998;19:743-751.
38. International Commission on Radiological Protection. *Radiological Protection in Biomedical Research.* ICRP Publication 62. Oxford, UK: Pergamon Press; 1993.

# Imaging infection/inflammation in the new millennium

Huub J.J.M. Rennen, Otto C. Boerman, Wim J.G. Oyen, Frans H.M. Corstens

Department of Nuclear Medicine, University Medical Center Nijmegen, P.O. Box 9101, 6500 HB Nijmegen, The Netherlands

Published online: 21 December 2000

© Springer-Verlag 2000

**Abstract.** In the closing half of the past century a wide variety of approaches were developed to visualise infection and inflammation by gamma scintigraphy. Use of autologous leucocytes, labelled with indium-111 or technetium-99m, is still considered the “gold standard” nuclear medicine technique for the imaging of infection and inflammation. However, the range of radiopharmaceuticals used to investigate infectious and non-microbial inflammatory disorders is expanding rapidly. Developments in protein/peptide chemistry and in radiochemistry should lead to agents with very high specific activities. Recently, positron emission tomography with fluorine-18 fluorodeoxyglucose has been shown to delineate infectious and inflammatory foci with high sensitivity. The third millennium will witness a gradual shift from basic (non-specific) or cumbersome, even hazardous techniques (radiolabelled leucocytes) to more sophisticated approaches. Here a survey is presented of the different approaches in use or under investigation.

**Keywords:** Imaging – Infection – Inflammation – Gamma scintigraphy – FDG-PET

**Eur J Nucl Med (2001) 28:241–252**

DOI 10.1007/s002590000447

## Introduction

Scintigraphic detection of infection and inflammation allows the determination of both the location and the number of infectious and inflammatory foci throughout the body. Since scintigraphic images are based on functional (physiological and/or biochemical) tissue changes, infectious and inflammatory foci can be visualised in

their early phases, when anatomical changes are not yet apparent. Over the past 30 years, a variety of approaches have been developed to visualise infection and inflammation using radionuclides and gamma cameras. Recently, positron emission tomography (PET) with fluorine-18 fluorodeoxyglucose (FDG) has been introduced in the field of infection/inflammation imaging. To understand the mode of action of many of these new agents, the pathophysiology of inflammation needs to be elucidated.

## Infection and inflammation

Inflammation can be described as the reaction of the body to any kind of injury [1]. Such injury ranges from trauma to ischaemia, to neoplasm, and also to invasion by micro-organisms, in which case we speak of infection. Infection simply means “contamination with micro-organisms”. There can be infection without inflammation, as in the case of a severely immunocompromised patient. Especially in such cases it is clear that for the purpose of imaging one would need an agent that directly interacts with the micro-organisms. Conversely, there can be inflammation without infection when tissue injury is not due to invasion by micro-organisms but rather is caused by “stimuli” such as trauma, ischaemia, neoplasm or foreign particles (e.g. asbestos).

## Components of the inflammatory response

The response to acute infection/inflammation is characterised by:

- Locally increased blood supply
- Increased vascular permeability in the affected area
- Enhanced transudation of plasma proteins
- Enhanced influx of leucocytes

In response to tissue damage, powerful defence mechanisms are activated, consisting of cells (leucocytes) and plasma proteins (opsonins, antibodies, complement). A complex variety of mediators, both vasoactive and chemotactic, are involved in the process. These mediators

Huub J.J.M. Rennen (✉)

Department of Nuclear Medicine,  
University Medical Center Nijmegen, P.O. Box 9101,  
6500 HB Nijmegen, The Netherlands  
e-mail: H.Rennen@nugen.azn.nl  
Tel.: +31-24-3615054, Fax: +31-24-3618942

are generated at the focus of inflammation/infection and amplify the local response by the recruitment of cells and plasma components from the blood. Vasodilatation and increased endothelial permeability are induced to facilitate the extravasation of proteins and cells. In addition, the expression of adhesion molecules on endothelial cells and leucocytes is stimulated. In this way, leucocytes migrate actively from the circulation into inflamed tissue. First, they adhere to the vascular endothelium due to locally enhanced expression of adhesion molecules (rolling, arrest and adhesion). Subsequently, they pass through the endothelium and the basal membrane (diapedesis) and migrate into the inflammatory focus (chemotaxis). In acute inflammation/infection, the infiltrating cells are predominantly polymorphonuclear cells (PMNs).

In chronic inflammation/infection, the cellular response is different from that in acute inflammation/infection. Infiltrating cells are predominantly mononuclear cells: lymphocytes, monocytes and macrophages.

### Non-specific and specific radiopharmaceuticals used to image infection

#### *Non-specific tracers of infection*

Increased blood supply, increased vascular permeability and enhanced transudation are processes that can be utilised for non-specific accumulation of tracers. It must be emphasised that all radiopharmaceuticals accumulate to some extent in this non-specific way at the site of infection. Examples of non-specific tracers for the detection of infection based on increased vascular permeability are:

- $^{67}\text{Ga}$  citrate
- Radiolabelled non-specific immunoglobulins
- Radiolabelled liposomes
- Radiolabelled avidin-biotin

#### *Specific tracers of infection*

Specific processes of accumulation comprise a number of possible interactions between the radiopharmaceutical and the target, e.g. receptor binding and antibody-antigen binding. Several pathways can be distinguished in infection imaging based on specific processes of accumulation of the radiopharmaceutical, as shown in Table 1. Leucocytes preferentially target infection by chemotaxis and can therefore be used to transport radionuclides to the infected area (pathway A). They move massively to the site of infection and localise there in great numbers. Detection of infection can be accomplished by direct labelling of leucocytes (ex vivo labelling) or by labelling leucocytes indirectly, i.e. in vivo. Ex vivo labelling requires withdrawal of blood from the patient, purification of leucocytes, and labelling and reinjection of the radiolabelled cells. Use of autologous leucocytes labelled with  $^{111}\text{In}$  or  $^{99\text{m}}\text{Tc}$  can lead to positive imaging because leucocytes, even after ex vivo labelling, have the capacity to migrate to the inflamed area. In vivo labelling of leucocytes can be based on antibody-antigen interactions (e.g. radiolabelled antigranulocyte monoclonal antibodies) or on leucocyte receptor binding (e.g. radiolabelled chemotactic peptides and cytokines). With respect to pathways B and C, vasoactive or chemotactic mediators of the inflammatory process either can be targeted in vivo by radiopharmaceuticals or can be radiolabelled in vitro and injected. So, either we label in vivo a particular

**Table 1.** Strategies in infection imaging with specific tracers

A	Target leucocytes moving to and present in the focus of infection: <ul style="list-style-type: none"> <li>– Direct labelling of leucocytes (ex vivo labelling)</li> <li>– Indirect labelling of leucocytes (in vivo labelling): <ul style="list-style-type: none"> <li>– Antibody-antigen interactions: radiolabelled antigranulocyte monoclonal antibodies/antibody fragments</li> <li>– Binding to receptors on leucocytes: <ul style="list-style-type: none"> <li>– Radiolabelled chemotactic peptides: formyl-Met-Leu-Phe</li> <li>– Radiolabelled cytokines: the interleukins, platelet factor 4</li> </ul> </li> </ul> </li> </ul>
B	Target mediators that are already present at or migrate to the site of infection by radiopharmaceuticals: <ul style="list-style-type: none"> <li>– Anti-E-selectin antibodies or anti-E-selectin <math>\text{F(ab')}_2</math> fragments</li> </ul>
C	Administer radiolabelled mediators that migrate to the site of infection: <ul style="list-style-type: none"> <li>– Radiolabelled mediators binding to leucocytes (see above: Indirect labelling of leucocytes)</li> </ul>
D	Target the locally present micro-organisms: <ul style="list-style-type: none"> <li>– Radiolabelled ciprofloxacin</li> <li>– Radiolabelled antimicrobial peptides</li> </ul>
E	Target the increased glucose uptake of infiltrated granulocytes and tissue macrophages: <ul style="list-style-type: none"> <li>– FDG-PET</li> </ul>

**Table 2.** Criteria for an ideal tracer

---

Efficient accumulation and good retention in inflammatory foci
Rapid clearance from the background
No accumulation in non-target organs
No toxicity
Early diagnostic imaging
Ready availability and low cost
Easy low-hazard preparation
Differentiation between infection and non-microbial inflammation
Low radiation burden

---

component that is already present in or goes to the inflamed area, or we inject in a radiolabelled form the mediator itself. Pathway D can be said truly to be infection imaging, in that radiopharmaceuticals are used that specifically target micro-organisms. A completely different mechanism of accumulation at the inflammatory site underlies PET scans using FDG, namely enhanced uptake of radiolabelled glucose by infiltrated granulocytes and tissue macrophages with increased metabolic requirements (pathway E). The accumulation of FDG in cells with increased glucose metabolism is specific. However, FDG is also taken up by, for example, tumour cells. So, accumulation of FDG is not specific for infection and inflammatory processes as such.

### Characteristics of the ideal conditions for infection imaging

During recent decades, many radiopharmaceuticals have been developed for the diagnosis of infection, each with its own advantages and disadvantages. Criteria for the ideal tracer are summarised in Table 2. It will be clear that no radiopharmaceutical meets all these criteria in a perfect way. In clinical practice the choice of the imaging agent is based on careful examination of each individual case. Early diagnostic imaging is preferable but not always necessary, as in the case of osteomyelitis or in infected bone/joint prostheses. A 1-day protocol is favourable in cases of severe and acute illness such as lung infections. Imaging with high radiation doses or imaging that entails the occurrence of minor transient side-effects after the administration of the radiopharmaceutical is in general unfavourable and should be considered only when significant clinical benefit is to be expected.

### Developing new tracers

For the development of new infection-imaging radiopharmaceuticals, the following route can be proposed. Once a potential new radiopharmaceutical has passed the laboratory level of synthesis, purification and quality control, in vitro and in vivo testing starts. If the potential new tracer is aimed at binding to certain cell types in

vivo (e.g. leucocytes, lymphocytes, bacteria), in vitro binding assays with the target cells can give an indication of the potential of the product. Target cells for binding studies can be isolated from the blood or cell lines can be generated bearing receptors from original cells by cDNA transfection techniques. Reproducibility of receptor binding assays is generally better using these cell cultures bearing the desired transfected receptors. In binding assays, the affinity and specificity of the agent for the target cells can be determined.

Subsequently, the new tracer can be tested in one of the simple and easy-to-use animal models of infection. Mice or rats with soft tissue infections induced by *Staphylococcus aureus* or *Escherichia coli* can serve as a good model for these first explorations. Biodistribution data generated in such a model can give a first impression of the imaging potential of the new tracer and allow the first comparison with known agents [2, 3]. Data on accumulation in the target (%ID/g), target/non-target ratios, blood clearance and the primary route of clearance (hepatobiliary/renal) can be obtained.

The next and in most cases the final step in preclinical testing will involve more advanced models of infection in animals of more closely related species like rabbits and dogs. High costs and strict legal regulations will in most cases impede the use of primates for these studies. Moreover, the new information that experiments in primates could reveal does not outweigh the investments in money and energy in general. Besides the soft tissue infection mentioned above, more complicated models of infection can be used, which are of more clinical relevance: colitis [4, 5], osteomyelitis [6, 7], endocarditis [8, 9], meningitis [10, 11] and respiratory tract infections [12, 13]. In many cases, these models require more specialised skills and experience. The model of choice depends on the intended application of the new tracer. In rabbit and dog model(s), a direct comparison between the new tracer and the “gold standard”  $^{111}\text{In}$ - or  $^{99\text{m}}\text{Tc}$ -labelled purified granulocytes can be carried out.

Once a new tracer has successfully passed these stages of laboratory and preclinical research, the agent should be tested in clinical trials in patients suspected of having infectious or inflammatory disease.

### Detection of infection by non-specific tracers

#### $^{67}\text{Ga}$ citrate

$^{67}\text{Ga}$  citrate is used in clinical practice in several pathological conditions, including infection and many skeletal disorders [14, 15]. Once injected in the circulation,  $^{67}\text{Ga}$  citrate binds to circulating transferrin. This complex extravasates at the site of infection owing to the locally enhanced vascular permeability [16], and is partly bound there to lactoferrin excreted by leucocytes or to siderophores produced by micro-organisms [17]. The agent is

excreted partly via the kidneys (especially during the first 24 h after injection), and via the gastrointestinal tract. Physiological uptake of the radiolabel occurs in liver, bone, bone marrow and bowel. Although  $^{67}\text{Ga}$  citrate scintigraphy has high sensitivity for both acute and chronic infection and non-infectious inflammation [18], there are several shortcomings that limit its clinical application. The specificity of the technique is low owing to physiological bowel excretion and accumulation in malignant tissues and areas of bone modelling [19, 20, 21]. In addition, the radiopharmaceutical has unfavourable imaging characteristics (long physical half-life and high-energy gamma radiation), causing high radiation absorbed doses. Furthermore, optimal imaging often requires delayed recordings up to 72 h. These unfavourable characteristics, in combination with the development of newer radiopharmaceuticals, have narrowed the clinical indication for gallium scintigraphy to certain conditions such as lung infections and chronic osteomyelitis [18, 21].

#### *Non-specific immunoglobulins*

Initially it was hypothesised that human polyclonal immunoglobulin (HIG) was retained in infectious foci owing to the interaction with Fc- $\gamma$  receptors as expressed on infiltrating leucocytes [22]. Later studies showed that radiolabelled HIG accumulates in infectious foci by non-specific extravasation due to the locally enhanced vascular permeability [23]. For clinical use, HIG has been labelled with  $^{111}\text{In}$  as well as  $^{99\text{m}}\text{Tc}$ . Both agents have slow blood clearance and physiological uptake in the liver, the spleen and the kidneys. The  $^{99\text{m}}\text{Tc}$ -labelled preparation has the known ideal radiation characteristics, while the  $^{111}\text{In}$ -labelled preparation allows imaging at time points beyond 24 h post injection.  $^{111}\text{In}$ - or  $^{99\text{m}}\text{Tc}$ -labelled HIG has been extensively tested in a large number of clinical studies. It has shown excellent performance in the localisation of musculoskeletal infection and inflammation [24]. In addition, good results have been reported in pulmonary infection – particularly in immunocompromised patients [25, 26] – and abdominal inflammation [27]. In a comparative study, Dams et al. showed that  $^{99\text{m}}\text{Tc}$ -HIG labelled via the  $^{99\text{m}}\text{Tc}$  chelator hydrazinonicotinamide (HYNIC) has in vivo characteristics highly similar to those of  $^{111}\text{In}$ -HIG, and in most cases can replace the  $^{111}\text{In}$ -labelled compound [28]. Poor sensitivity of radiolabelled HIG is found in the diagnosis of endocarditis and vascular lesions in general, owing to long-lasting high levels of circulating activity. A general limitation is the long time span between injection and final diagnosis (24–48 h).

#### *Liposomes*

Liposomes are spheres consisting of one or more lipid bilayers surrounding an aqueous space. They were proposed as vehicles to image infection some 20 years ago, but the preparations used in those early years were cleared from the circulation very rapidly by the mononuclear/phagocyte system (MPS). However, if the surface of the liposomes is coated with a hydrophilic polymer such as polyethylene glycol (PEG), they circumvent recognition by the MPS, leading to a prolonged residence time in the circulation and enhanced uptake at pathological sites by extravasation due to locally enhanced vascular permeability [29]. Such stabilised PEG-liposomes can be labelled with  $^{111}\text{In}$ -oxinate and with  $^{99\text{m}}\text{Tc}$  either using hexamethylpropylene amine oxime (HMPAO) as an internal label or via HYNIC as an external chelator. Labelling is easy and takes only minutes [30]. The first clinical evaluation showed good imaging of focal infection [31]. In patients suspected of harbouring infectious or inflammatory disease,  $^{99\text{m}}\text{Tc}$ -PEG-liposomes were directly compared with  $^{111}\text{In}$ -IgG scintigraphy.  $^{99\text{m}}\text{Tc}$ -PEG-liposome scintigraphy showed high sensitivity (94%) and specificity (89%). Visualisation of musculoskeletal and abdominal pathology was better than with  $^{111}\text{In}$ -IgG. Unfortunately, in another clinical study, self-limiting side-effects were observed in three out of nine patients [32].

#### *The avidin-biotin system*

Avidins are a family of proteins present in the eggs of amphibians, reptiles and birds; streptavidin is a member of the same family. Avidin and streptavidin (mol. wt. 66,000 and 60,000, respectively) bind to biotin with extremely high affinity ( $K_d=10^{-15}$  M). Biotin is a compound of low molecular weight that can be radiolabelled. The avidin-biotin approach is based on the fact that avidin (or streptavidin) will non-specifically localise at sites of infection owing to increased vascular permeability. Avidin (or streptavidin) is injected as a pretargeting agent, followed hours later by a second injection with radiolabelled biotin [33]. Good diagnostic accuracy was demonstrated in studies of vascular infection [34] and chronic osteomyelitis [35].

#### *Limitations in the use of non-specific tracers to image infections*

Infectious foci can be visualised with tracers without a specific interaction between the agent and a tissue component in the infectious focus, in a non-specific process of localisation due to the locally enhanced vascular permeability. Extravasation of (macro)molecules via diffusion is a slow process. Prolonged high blood levels are

**Table 3.** Overview of studies in infection imaging with new specific tracers (including FDG)

Agent	No. of patients studied	Year of publication	References
Antigranulocyte antibodies:			
Anti-NCA-95: BW 250/183	>300	1989–2000	[42, 43, 44, 45, 46, 47, 48]
Anti-CD66: LeukoScan	>100	1994–2000	[49, 50, 51]
Anti-CD15: LeuTech	>200	1996–2000	[52, 53, 54, 55]
Chemotactic peptide analogues	Preclinical	1991–1997	[59, 60, 61, 62, 63]
Interleukin-1ra	5	2000	[66]
Interleukin-2	>400	1999, 2000	[69, 70, 71]
Interleukin-8	8	1996–2000	[3, 72, 73, 74]
PF-4 derivative: P483H	30	1996, 1999	[75, 76]
Anti E-selectin antibodies	25	1996–1997	[80, 81]
Ciprofloxacin: Infecton	>1000	1996–2000	[82, 83]
Neutrophil defensins: HNP-1	Preclinical	1998, 1999	[84, 85]
FDG (PET)	>250	1996–2000	[91, 92, 93, 94, 95, 96, 97, 98]

needed to allow (sufficient) diffusion into the target tissue. However, high blood levels entail relatively high background levels, especially in well-perfused tissues. Secondly, in chronic inflammation the vascular permeability tends to normalise. Furthermore, because non-specific agents accumulate owing to a common feature of infection and inflammation, these agents cannot distinguish between infection and inflammation. As a result, non-specific tracers are in principle limited in their ability to detect (and discriminate between) infections and inflammations. In this respect,  $^{67}\text{Ga}$  citrate, radiolabelled HIG, radiolabelled liposomes and the avidin-biotin approach face the same inherent limitations.

### Detection of infection by specific tracers

As outlined in Table 1, different strategies in imaging infection using specific tracers can be employed. These agents will be presented in more detail. An overview of agents that are currently being developed for infection imaging is presented in Table 3.

### Detection of infection by direct labelling of leucocytes

Ex vivo labelled autologous leucocytes were developed in the 1970s and 1980s [36, 37, 38] and their use is still considered the “gold standard” nuclear medicine technique for infection and inflammation imaging. After intravenous administration, there is initial sequestration of the labelled leucocytes in the lungs, with subsequent rapid clearance of the activity from the lungs. The radiolabel rapidly clears from the blood and in most cases there is high uptake in granulocytic infiltrates, while a substantial portion of the leucocytes (presumably the damaged cells) accumulate in the spleen. Thus, as a radiopharmaceutical, radiolabelled leucocytes are a spe-

cific indicator for leucocytic infiltration, but not for infection. McAfee and Thakur developed a technique to label autologous leucocytes with  $^{111}\text{In}$  using oxinate as a chelate to transfer the radiolabel into the cell [36]. Peters et al. developed a labelling technique using HMPAO, a lipophilic chelator, that allows efficient labelling of white blood cells with  $^{99\text{m}}\text{Tc}$  [37]. In contrast to  $^{111}\text{In}$ -oxinate, some of the  $^{99\text{m}}\text{Tc}$ -HMPAO is released from the leucocytes after injection and subsequently is excreted renally (within minutes) and via the hepatobiliary system (after hours) [38]. Due to the more optimal radiation characteristics,  $^{99\text{m}}\text{Tc}$ -labelled leucocytes have replaced  $^{111}\text{In}$ -labelled leucocytes for most indications. For evaluation of kidney, bladder and gall-bladder infections, the use of leucocytes labelled with  $^{111}\text{In}$  is preferred. The excellent performance of radiolabelled leucocytes for imaging infection and inflammation was demonstrated in a series of studies: for imaging infectious/inflammatory foci, sensitivity exceeded 95% [38, 39]. There was some concern that more chronic infections could be missed with labelled leucocyte scans, because such infections generate a smaller granulocyte response than acute infections. However, a study in 155 patients showed that the sensitivity of labelled leucocytes for the detection of acute infections (90%) was not significantly different from the sensitivity for the detection of chronic infections (86%) [40]. With regard to diagnostic accuracy, there is no need for a better imaging agent than labelled autologous leucocytes. However, the preparation of this radiopharmaceutical is laborious, requires specialised equipment and can be hazardous. Isolating and labelling a patient's white blood cells takes a trained technician approximately 3 h. In addition, the need to handle potentially contaminated blood can lead to transmission of blood-borne pathogens such as HIV and HBV [41].

## Detection of infection by in vivo labelling of leucocytes

A gross distinction can be drawn between tracers that bind leucocytes by receptor binding (relatively small molecules, of molecular weight <20,000) and tracers that bind leucocytes by antibody-antigen interaction (relatively large molecules). The antibodies range in molecular weight from 50,000 (antibody fragments) through 150,000 (IgG) to 900,000 (IgM).

### *Antigranulocyte antibodies and antibody fragments*

Ever since it became clear that radiolabelled autologous leucocytes could visualise infectious foci, investigators have tried to develop a method that would label leucocytes in the circulation or in the infectious foci. Instead of isolating the white blood cells from a patient and labelling the cells *ex vivo*, these methods aim to label white blood cells *in vivo*. Labelling procedures are easier and do not require handling of potentially contaminated blood. The use of radiolabelled monoclonal antibodies against surface antigens as present on granulocytes was one of the first attempts to accomplish *in vivo* labelling of leucocytes. Several monoclonal antibodies reactive with antigens expressed on granulocytes (NCA, CD15, CD66 and CD67) have been developed. At least three anti-granulocyte antibodies have been tested for infection imaging: anti-NCA-95 IgG (BW250/183) [42, 43, 44, 45, 46, 47, 48], anti-NCA-90 Fab' (Immu-MN3, LeukoScan: anti-CD66) [49, 50, 51], and anti-SSEA-1 IgM (LeuTech: anti-CD15) [52, 53, 54, 55]. Each of these anti-granulocyte antibodies labelled with  $^{99m}\text{Tc}$  or  $^{123}\text{I}$  allowed accurate delineation of infection.

It was soon realised that the *in vivo* behaviour of these labelled anti-granulocyte antibody preparations did not mimic the behaviour of radiolabelled leucocytes. In general, blood clearance of the IgG preparations was much slower, giving a high background radioactivity that decreased slowly with time. For that reason, the time interval between injection of the labelled antibodies and the acquisition of images that was required in order to obtain good target-background ratios was relatively long. Furthermore, no initial lung entrapment was seen and splenic uptake was much lower, while the preparations based on antibody fragments (Fab, Fab') had a much higher renal excretion. Similarly, the IgM antibody had a much higher liver uptake as compared with the *ex vivo* labelled white blood cells. Becker et al. showed that less than 10% of the radiolabelled BW250/183 antibody present in the blood was actually associated with granulocytes [42]. These observations indicated that the anti-granulocyte antibody approach for infection imaging, although feasible, did not represent a method for the labelling of white blood cells *in vivo*. It is now generally accepted that radiolabelled anti-granulocyte antibodies

localise in infectious foci mainly by non-specific extravasation due to the locally enhanced vascular permeability, and that binding of the antibody to infiltrated leucocytes in the inflamed tissue may contribute to the retention of the radiolabel in the focus. Perhaps an exception should be made for anti-SSEA-1 IgM (LeuTech: anti-CD15) [52]. This antibody recognises CD-15 antigens on PMNs with high affinity ( $K_d=10^{-11}\text{ M}$ ) and the *in vivo* PMN binding exceeds 50%, pointing towards the involvement of more specific processes in accumulation in infected tissue. Recently, a  $^{99m}\text{Tc}$ -labelled anti-CD15 IgM monoclonal antibody has shown promising results in patients with equivocal appendicitis [53].

The anti-granulocyte antibody-based radiopharmaceuticals visualised infectious foci in patients with a sensitivity between 80% and 90% [56].  $^{99m}\text{Tc}$ -BW250/183 scintigraphy was useful in the evaluation of vascular graft infection and prosthetic heart valve infection. Good results were also obtained in the evaluation of patients with inflammatory bowel disease [43, 56], although the agent appeared to be less accurate than labelled leucocytes [45, 46]. Pulmonary infections – with the exception of lung abscesses – were not visualised. Peripheral bone infections were adequately visualised, but the sensitivity decreased when the focus was located closer to the spine [50]. Due to the relatively slow blood clearance of the agent, a 24-h post-injection scan is generally necessary for correct localisation of the inflammatory focus. A major disadvantage of the murine monoclonal antibodies is that they may induce human anti-mouse antibodies, which can result in altered biodistribution after subsequent injections [56, 57]. In this respect, the use of antibody fragments instead of the whole antibody seems to be more advantageous, since such fragments appear to be less immunogenic [56]. In addition, antibody fragments show faster blood clearance and may thus provide earlier diagnosis. The  $^{99m}\text{Tc}$ -labelled antigranulocyte Fab' fragment (LeukoScan) has been registered in Europe as an infection imaging agent [49]. Further clinical studies will help to define the utility of these new agents in clinical practice.

### *Chemotactic peptides*

Like anti-granulocyte antibodies, peptides with high affinity for receptors expressed preferentially on granulocytes could be suitable for targeting granulocytes *in vivo*. A wide variety of peptides that bind to receptors expressed on white blood cells have been tested for the detection of infection. One of the first receptor-binding peptides that was tested for its ability to image infectious foci was the chemotactic peptide formyl-Met-Leu-Phe. This tripeptide, which is N-terminally formylated, is a chemotactic factor produced by bacteria. It binds to receptors on granulocytes and monocytes with high affinity ( $K_d=10\text{--}30\text{ nM}$ ). The first work on this radiolabelled



chemotactic peptide was reported almost 20 years ago. Zoghbi et al. and later McAfee et al. labelled f-Met-Leu-Phe and investigated its *in vivo* characteristics [58]. They found that even low doses of peptide induced a transient granulocytopenia. In 1991, Fischman et al. described the synthesis of four DTPA-derivatised chemotactic peptide analogues and their labelling with  $^{111}\text{In}$  [59]. All peptides maintained biological activity and receptor binding affinity. The peptides were tested in rats with *Escherichia coli* infections. All analogues showed preferential localisation in the focal infection within 1 h after injection. In a comparative study in rabbits with *E. coli* infections, it was demonstrated that localisation of infection using  $^{99\text{m}}\text{Tc}$ -labelled f-Met-Leu-Phe was superior to that using  $^{111}\text{In}$ -labelled leucocytes [60]. However, although a high specific activity  $^{99\text{m}}\text{Tc}$ -labelling method was applied, a peptide dose as low as 10 ng/kg still had an effect on the peripheral leucocyte counts [61]. Several antagonists were developed to circumvent this undesirable biological activity of the radiolabelled chemotactic peptide. However, these antagonists had lower uptake in the infectious focus, most likely owing to reduced affinity for the receptor [62, 63]. In summary, rapid imaging of infection and inflammation is feasible with radiolabelled chemotactic peptides; however, the undesired biological side-effects of these peptides seem to impede further clinical development.

### Cytokines

Labelled cytokines are an interesting class of protein radiopharmaceuticals of low molecular weight (<20,000). Cytokines act through an interaction with specific cell-surface receptors expressed on known cell populations. Binding affinities are usually high (nanomolar range). Cytokine receptors are expressed at low levels on non-excited cells, but their expression can be upregulated during activation.

#### Interleukin-1

Interleukin 1 (IL-1) binds receptors expressed mainly on granulocytes, monocytes and lymphocytes, with high affinity. Studies in mice with focal *Staphylococcus aureus* infections showed specific uptake of radio-iodinated IL-1 at the site of infection [2]. Using IL-1 receptor blocking antibodies, it could be demonstrated that accumulation of the agent in the infectious foci was due to binding to the IL-1 type II receptor [64]. Unfortunately, the biological effects (e.g. hypotension, headache) of IL-1 even at very low doses (10 ng/kg) precluded clinical application of radiolabelled IL-1. Therefore, the naturally occurring IL-1 receptor antagonist (IL-1ra) was tested as an imaging agent. This equally sized (17 kDa) protein binds IL-1 receptors with similar high affinity

but lacks any biological activity. In a comparative study in rabbits with focal *E. coli* infections, the abscess uptake of radio-iodinated IL-1ra was half that of radio-iodinated IL-1 [65].  $^{123}\text{I}$ -IL-1ra was tested in patients with rheumatoid arthritis. In these patients, inflamed joints were nicely visualised; however, major retention of the radiolabel in the intestinal tract indicated that this agent cannot be used to visualise infectious and inflammatory lesions in the abdomen [66].

#### Interleukin-2

Chronic inflammation is characterised by infiltration of the target tissue by lymphocytes. These infiltrates have been successfully targeted with radiolabelled interleukin-2 (IL-2). The IL-2 is considered to bind specifically to IL-2 receptors expressed on activated T lymphocytes. In a study in an animal model of human auto-immune diabetes mellitus, Signore et al. showed that lymphocytic infiltration in the pancreas could be visualised with  $^{123}\text{I}$ -labelled IL-2 between 5 and 15 min after injection [67]. A method was developed that allowed the preparation of a  $^{99\text{m}}\text{Tc}$ -IL-2 preparation with a high specific activity [68]. Studies in patients with chronic inflammatory conditions, including insulin-dependent diabetes, Hashimoto's thyroiditis, Graves' disease, Crohn's disease, coeliac disease and other auto-immune diseases, demonstrated localisation of  $^{123}\text{I}$ - or  $^{99\text{m}}\text{Tc}$ -labelled IL-2 at the site of lymphocytic infiltration [69, 70, 71]. These results suggest that radiolabelled IL-2 might be a suitable agent for *in vivo* targeting of mononuclear cell infiltration as present in auto-immune diseases.

#### Interleukin-8

Interleukin-8 (IL-8) is a small protein (8.5 kDa) belonging to the CXC subfamily of the chemokines, or chemotactic cytokines, in which the first two cysteine residues are separated by one amino acid residue. IL-8 binds to receptors on neutrophils with high affinity (0.3–4 nM). Hay and colleagues [72] studied the *in vivo* behaviour of radio-iodinated IL-8 in a rat model with carrageenan-induced sterile inflammation. The uptake peaked at 1–3 h after injection and declined thereafter. Target-to-background ratios remained relatively low. In a pilot study in eight patients, these investigators showed that  $^{123}\text{I}$ -IL-8 could visualise inflammatory foci [73]. The labelling method appeared to have major effects on the *in vivo* biodistribution of radio-iodinated IL-8. The scintigraphic imaging characteristics of IL-8 labelled via the Bolton-Hunter method were clearly superior to those of IL-8 labelled via the iodogen method, despite similar *in vitro* cell binding characteristics [3]. In rabbits with focal *E. coli* infection, accumulation of  $^{123}\text{I}$ -labelled IL-8 in the abscess was rapid and high. The specific activity of

this IL-8 preparation was relatively low, resulting in a transient reduction in peripheral leucocyte counts to 45% after a dose of 25 µg/kg  $^{123}\text{I}$ -IL-8, followed by leukocytosis (170% of pre-injection level) for several hours. Recently, a  $^{99\text{m}}\text{Tc}$ -labelled IL-8 preparation was developed using HYNIC as a chelator. In rabbits with *E. coli* infection, high abscess uptake of  $^{99\text{m}}\text{Tc}$ -HYNIC-IL-8 and high abscess-to-background ratios were obtained compared with those obtained using the radio-iodinated preparation [74]. The higher specific activity of the  $^{99\text{m}}\text{Tc}$ -labelled IL-8 preparation ameliorates concerns about the influence on WBC counts.

#### *Platelet factor 4*

Platelet factor 4 (PF-4), like IL-8, is a member of the CXC chemokines. PF-4 binds the CXC type II (= IL-8 type B) receptors expressed on neutrophils and monocytes. PF-4 has been called the “body’s heparin neutralising agent”. At Diatide Inc., the peptide P483H was synthesised. This peptide contains the heparin-binding region of PF-4 – complexed with heparin – and a lysine-rich sequence to facilitate rapid renal clearance. In a rabbit model of infection,  $^{99\text{m}}\text{Tc}$ -P483H clearly delineated the infectious foci as early as 4 h after injection. No systemic side-effects were observed: the transient neutropenia observed with IL-8 and f-Met-Leu-Phe was not encountered after i.v. injection of P483H [75].  $^{99\text{m}}\text{Tc}$ -P483H has been studied in patients to test its applicability as an imaging agent for scintigraphic detection of infection and inflammation, with fair results (82% sensitivity, 77% specificity) [76]. However, in some patients excessive thyroid uptake was observed, suggesting the release of  $^{99\text{m}}\text{Tc}$  from the agent in vivo.

### **Detection of infection by targeting adhesion molecules using anti-E-selectin antibodies**

E-selectin is an endothelial adhesion molecule exclusively expressed on the luminal surface of activated endothelial cells and capable of binding to leucocytes. Radio-labelled anti-E-selectin monoclonal antibodies [77] or anti-E-selectin  $\text{F(ab')}_2$  fragments [78] have been successfully used to image arthritis and chronic inflammatory bowel disease [79, 80, 81]. To overcome the possible induction of human anti-mouse antibodies, a bioengineered single-chain antibody construct has been developed.

### **Detection of infection by radiolabelled antibiotics**

#### *Ciprofloxacin (Infecton)*

None of the agents discussed above can make a differential diagnosis between infection and inflammation as

they accumulate in the focus owing to a common feature of infection and inflammation. Ciprofloxacin, a fluoroquinolone antimicrobial agent, binds to the DNA gyrase enzyme present in all dividing bacteria, even to those resistant to ciprofloxacin. Fluoroquinolones are thought neither to bind to dead bacteria nor to accumulate in non-microbial inflammatory processes such as Crohn’s disease. It is claimed that with these  $^{99\text{m}}\text{Tc}$ -labelled agents it is possible to discriminate between infection and sterile inflammation [82]. First clinical studies in several centres have shown high accuracy in the detection of bacterial infection. Data on the efficacy of  $^{99\text{m}}\text{Tc}$ -Infecton imaging in 90 patients with suspected infective disorders reveal a sensitivity of 70% and a specificity of 93% [83]. Since this agent is not taken up in bone marrow, it could be very helpful in the evaluation of infection of orthopaedic prostheses.

#### *Antimicrobial peptides*

Neutrophil defensins (human neutrophil peptides, HNPs) are stored in the granules of neutrophils. In addition to their direct antimicrobial activity, the peptides have chemo-attractive activity for various monocytes and lymphocytes. It has been hypothesised that their cationic charge facilitates binding of these peptides to various micro-organisms. HNP-1 was labelled with  $^{99\text{m}}\text{Tc}$  using a direct method by reducing the disulphide bridges of the molecule. Using this agent in experimental thigh infections in mice, abscess-to-background ratios were low and decreased with time [84, 85]. In the peritoneal cavity of the infected mice,  $^{99\text{m}}\text{Tc}$ -HNP-1 bound to bacteria rather than to leucocytes. However, this agent needs extensive optimisation and tailoring to enable it to distinguish between bacterial infection and sterile inflammation.

### **Detection of infection by FDG-PET**

The use of  $^{18}\text{F}$ -fluorodeoxyglucose positron emission tomography (FDG-PET) has become increasingly important for differentiating malignant from benign tumours, for tumour staging and for evaluating treatment efficacy in cancer patients [86, 87]. As early as 1931, Warburg demonstrated an increased glucose metabolism in malignant tumours in vitro [88]. FDG accumulates quantitatively in malignant tumours in vivo mainly because of their increased glucose metabolism. However, during the staging and follow-up of malignant tumours, false-positive findings occasionally occur, mainly due to infectious or granulomatous processes [89]. Ever since Tahara et al. first demonstrated high FDG uptake in human abdominal abscesses in 1989 [90], FDG has been reported to accumulate in various inflammatory processes. Infection imaging with FDG-PET is based on the fact that granulocytes and macrophages use glucose as an energy source.

When activated through infection, metabolism and thus FDG uptake increases. The usefulness of FDG-PET for the imaging of infections has recently been demonstrated in several patient studies (Table 3) [91, 92, 93, 94, 95, 96, 97, 98]. FDG-PET has been studied in a wide variety of infections, including lesions of bacterial, tuberculous or fungal origin, soft tissue infections and bone infections. Sensitivity and specificity have generally exceeded 90%. FDG-PET has been especially successful in cases of osteomyelitis [93, 95, 96, 97, 98]. The high spatial resolution allows differentiation between osteomyelitis or inflammatory spondylitis and infection of the soft tissue surrounding the bone [97]. High spatial resolution and rapid accumulation into infectious foci are significant advantages over conventional imaging techniques such as the use of labelled leucocytes. However, the fact that uptake occurs in any cell type with high glycolytic activity is a serious limitation of the use of FDG-PET for infection imaging, restricting its specificity. For example, FDG-PET does not allow discrimination between tumour lesions and inflammatory lesions. Depending on the clinical setting, this may restrict the usefulness of FDG-PET in the imaging of infection. Moreover, FDG uptake in infectious foci is affected by serum glucose levels and by conditions such as diabetes mellitus. Cost is another issue. FDG-PET is a rather expensive imaging modality, and prospective studies in various patient populations will have to show the cost-effectiveness of FDG-PET for the imaging of inflammatory and infectious diseases.

## Conclusion

In the third millennium we will face a gradual shift in the field of nuclear medicine from basic (non-specific) and cumbersome, even hazardous techniques (radiolabelled leucocytes) to more intelligent approaches based on small agents that bind to their targets with high affinity. Classes of agents will be designed to specifically distinguish between infection and non-infectious inflammation and between acute and chronic processes. The advantages of  $^{99m}\text{Tc}$  as a radionuclide will be fully explored. Labelling with high specific activity will reduce the doses used, so that undesirable agonistic activities will become non-existent. In a totally different approach, undesirable agonistic activities will be alleviated by chemical modification of the agonist. Furthermore,  $^{18}\text{F}$ -FDG PET may prove to be as useful in the rapid detection and management of human infections as it is in the management of malignant diseases.

## References

1. Roitt IM. *Essential immunology*, 9th edn. Oxford: Blackwell Scientific, 1997.
2. van der Laken CJ, Boerman OC, Oyen WJG, van de Ven MTP, Claessens RAMJ, van der Meer JWM, Corstens FHM. Specific targeting of infectious foci with radioiodinated human recombinant interleukin-1 in an experimental model. *Eur J Nucl Med* 1995; 22:1249–1255.
3. van der Laken CJ, Boerman OC, Oyen WJG, van de Ven MTP, van der Meer JWM, Corstens FHM. Radiolabeled interleukin-8: scintigraphic detection of infection within a few hours. *J Nucl Med* 2000; 41:463–469.
4. Rogler G, Andus T. Cytokines in inflammatory bowel disease. *World J Surg* 1998; 22:382–389.
5. Neurath M, Fuss I, Strober W. TNBS-colitis. *Int Rev Immunol* 2000; 19:51–62.
6. Smeltzer MS, Thomas JR, Hickmon SG, Skinner RA, Nelson CL, Griffith D, Parr TR Jr, Evans RP. Characterization of a rabbit model of staphylococcal osteomyelitis. *J Orthop Res* 1997; 15:414–421.
7. Dams ET, Nijhof MW, Boerman OC, Laverman P, Storm G, Buma P, Lemmens JA, van der Meer JW, Corstens FH, Oyen WJ. Scintigraphic evaluation of experimental chronic osteomyelitis. *J Nucl Med* 2000; 41:896–902.
8. Veltrop MH, Bancsi MJ, Bertina RM, Thompson J. Role of monocytes in experimental *Staphylococcus aureus* endocarditis. *Infect Immun* 2000; 68:4818–4821.
9. Hershsberger E, Coyle EA, Kaatz GW, Zervos MJ, Rybak MJ. Comparison of a rabbit model of bacterial endocarditis and an in vitro infection model with simulated endocardial vegetations. *Antimicrob Agents Chemother* 2000; 44:1921–1924.
10. Koedel U, Pfister HW. Models of experimental bacterial meningitis. Role and limitations. *Infect Dis Clin North Am* 1999; 13:549–577.
11. Sorensen KN, Sobel RA, Clemons KV, Pappagianis D, Stevens DA, Williams PL. Comparison of fluconazole and itraconazole in a rabbit model of coccidioidal meningitis. *Antimicrob Agents Chemother* 2000; 44:1512–1517.
12. Dei-Cas E, Brun-Pascaud M, Bille-Hansen V, Allaert A, Aliouat EM. Animal models of pneumocystosis. *FEMS Immunol Med Microbiol* 1998; 22:163–168.
13. Cere N, Polack B. Animal pneumocystosis: a model for man. *Vet Res* 1999; 30:1–26.
14. Lavender JP, Lowe J, Barker JR, Burn JI, Chaudhri MA. Gallium 67 citrate scanning in neoplastic and inflammatory lesions. *Br J Radiol* 1971; 44:361–366.
15. Staab EV, McCartney WH. Role of gallium-67 in inflammatory disease. *Semin Nucl Med* 1978; 8:219–234.
16. Tsan MF. Mechanism of gallium-67 accumulation in inflammatory lesions. *J Nucl Med* 1985; 26:88–92.
17. Weiner R. The role of transferrin and other receptors in the mechanism of  $^{67}\text{Ga}$  localization. *Int J Rad Appl Instrum B* 1990; 17:141–149.
18. Palestro CJ. The current role of gallium imaging in infection. *Semin Nucl Med* 1994; 24:128–141.
19. Perkins PJ. Early gallium-67 abdominal imaging: pitfalls due to bowel activity. *Am J Roentgenol* 1981; 136:1016–1017.
20. Bekerman C, Hoffer PB, Bitran JD. The role of gallium-67 in the clinical evaluation of cancer. *Semin Nucl Med* 1984; 14: 296–323.
21. Seabold JE, Nepola JV, Conrad GR, et al. Detection of osteomyelitis at fracture nonunion sites: comparison of two scintigraphic methods. *Am J Roentgenol* 1989; 152:1021–1027.
22. Fischman AJ, Rubin RH, White JA, Locke E, Wilkinson RA, Nedelman M, Callahan RJ, Khaw BA, Strauss HW. Localization of Fc and Fab fragments of nonspecific polyclonal IgG at focal sites of inflammation. *J Nucl Med* 1990; 31:1199–1205.

23. Fischman AJ, Fucello AJ, Pellegrino-Gensey JL, Geltofsky J, Yarmush ML, Rubin RH, Strauss HW. Effect of carbohydrate modification on the localization of human polyclonal IgG at focal sites of bacterial infection. *J Nucl Med* 1992; 33: 1378–1382.
24. Nijhof MW, Oyen WJ, van Kampen A, Claessens RA, van der Meer JW, Corstens FHM. Evaluation of infections of the locomotor system with indium-111-labelled human IgG scintigraphy. *J Nucl Med* 1997; 38:1300–1305.
25. Oyen WJG, Claessens RAMJ, Raemaekers JMM, de Pauw BE, van der Meer JWM, Corstens FHM. Diagnosing infection in febrile granulocytopenic patients with indium-111 labeled human IgG. *J Clin Oncol* 1992; 10:61–68.
26. Buscombe JR, Oyen WJG, Grant A, et al. Indium-111-labeled human polyclonal immunoglobulin: identifying focal infection in patients positive for human immunodeficiency virus (HIV). *J Nucl Med* 1993; 34:1621–1625.
27. Mairal L, Lima PD, Martin Comin J, et al. Simultaneous administration of <sup>111</sup>In-human immunoglobulin and <sup>99m</sup>Tc-HMPAO labelled leukocytes in inflammatory bowel disease. *Eur J Nucl Med* 1995; 22:664–670.
28. Dams ET, Oyen WJ, Boerman OC, Claessens RA, Wymenga AB, van der Meer JW, Corstens FHM. Technetium-99m labeled to human immunoglobulin G through the nicotinyl hydrazine derivative: a clinical study. *J Nucl Med* 1998; 39: 1119–1124.
29. Boerman OC, Storm G, Oyen WJG, van Bloois L, van der Meer JWM, Claessens RAMJ, Corstens FHM. Sterically stabilized liposomes labeled with <sup>111</sup>In to image focal infection in rats. *J. Nucl. Med* 1995; 36:1639–1644.
30. Laverman P, Dams ETM, Oyen WJG, Storm G, Koenders EB, Prevost R, van der Meer JWM, Corstens FHM, Boerman OC. A novel method to label liposomes with Tc-99m via the hydrazino nicotinyl derivative: a comparison with Tc-99m-HMPAO-labeled PEG-liposomes. *J Nucl Med* 1999; 40:192–197.
31. Dams ETM, Oyen WJG, Boerman OC, Laverman P, Meeuwis APM, Koenders EB, Buijs WCAM, Storm G, Bakker J, van der Meer JWM, Corstens FHM. Tc-99m-PEG-liposomes for the scintigraphic detection of infection and inflammation: clinical evaluation. *J Nucl Med* 2000; 41:622–630.
32. Brouwers AH, de Jong DJ, Dams ETM, et al. Tc-99m-PEG-liposomes for the evaluation of colitis in Crohn's disease. *J Drug Targeting* 2000 (in press).
33. Hnatowich D, Virzi F, Rusckowski M. Investigation of avidin and biotin for imaging investigation. *J Nucl Med* 1987; 28: 1294–1302.
34. Samuel A, Paganelli G, Chiesa R, et al. Detection of prosthetic vascular graft infection using avidin/indium-111-biotin scintigraphy. *J Nucl Med* 1996; 37:55–61.
35. Rusckowski M, Paganelli, Hnatowich D, et al. Imaging osteomyelitis with streptavidin and indium-111-labeled biotin. *J Nucl Med* 1996; 37:1655–1662.
36. McAfee JG, Thakur ML. Survey of radioactive agents for the in vitro labeling of phagocytic leucocytes. I. Soluble agents. II. Particles. *J Nucl Med* 1976; 17:480–492.
37. Peters AM, Danpure HJ, Osman S, et al. Preliminary clinical experience with <sup>99m</sup>Tc-hexamethylpropylene-amineoxime for labelling leucocytes and imaging infection. *Lancet* 1986; II:945–949.
38. Peters AM. The utility of [<sup>99m</sup>Tc]HMPAO-leukocytes for imaging infection. *Semin Nucl Med* 1994; 24:110–127.
39. Datz FL. Indium-111-labeled leukocytes for the detection of infection: current status. *Semin Nucl Med* 1994; 24:92–109.
40. Datz FL, Thorne DA. Effect of chronicity of infection on the sensitivity of the In-111-labeled leukocyte scan. *AJR Am J Roentgenol* 1986; 147:809–812.
41. Lange JMA, Boucher CAB, Hollak CEM, Wiltink EH, Reiss P, van Royen EA, Roos M, Danner SA, Goudsmit J. Failure of zidovudine prophylaxis after accidental exposure to HIV-1. *N Engl J Med* 1990; 323:915–916.
42. Becker W, Borst U, Fischbach W, Paurka B, Schafer R, Borner W. Kinetic data of in vivo labelled granulocytes in humans with a murine Tc-99m-labelled monoclonal antibody. *Eur J Nucl Med* 1989; 15:361–366.
43. Becker W, Saptogino A, Wolf F. The single late Tc-99m granulocyte antibody scan in inflammatory diseases. *Nucl Med Commun* 1992; 13:186–192.
44. Schubiger PA, Hasler PH, Novak-Hofer I, Blauenstein P. Assessment of the binding properties of Granulosint. *Eur J Nucl Med* 1989; 15:605–608.
45. Papos M, Nagy F, Narai G, et al. Anti-granulocyte immunoscintigraphy and [<sup>99m</sup>Tc]hexamethylpropyleneamine-oxime-labeled leukocyte scintigraphy in inflammatory bowel disease. *Dig Dis Sci* 1996; 41:412–420.
46. Segarra I, Roca M, Baliellas L, et al. Granulocyte specific monoclonal antibody technetium-99m-BW 250/183 and indium-111 oxine labelled leukocyte scintigraphy in inflammatory bowel disease. *Eur J Nucl Med* 1991; 18:715–719.
47. Krause T, Reinhardt M, Nitzsche E, Moser E. Photopenic lesions in bone marrow scintigraphy using technetium-99m labeled antigranulocyte antibody without known tumour. *Nuklearmedizin* 1999; 38:85–89.
48. Gyorke T, Duffek L, Bartfai K, Mako E, Karlinger K, Mester A, Tarjan Z. The role of nuclear medicine in inflammatory bowel disease. A review with experiences of aspecific bowel activity using immunoscintigraphy with <sup>99m</sup>Tc anti-granulocyte antibodies. *Eur J Radiol* 2000; 35:183–192.
49. Becker W, Palestro CJ, Winship J, Feld T, Pinsky CM, Wolf F, Goldenberg DM. Rapid imaging of infections with a monoclonal antibody fragment (Leukoscan). *Clin Orthop* 1996; 329: 263–272.
50. Becker W, Bair J, Behr T, et al. Detection of soft-tissue infections and osteomyelitis using a technetium-99m labelled anti granulocyte monoclonal antibody fragment. *J Nucl Med* 1994; 35:1436–1443.
51. Gratz S, Raddatz D, Hagenah HG, Behr TM, Behe M, Becker W. <sup>99m</sup>Tc-labelled antigranulocyte monoclonal antibody Fab' fragments versus echocardiography in the diagnosis of subacute infective endocarditis. *Int J Cardiology* 2000; 75:75–84.
52. Thakur ML, Marcus CS, Henneman P, Butler J, Sinow R, Diggles L, Minami C, Mason G, Klein S, Rhodes B. Imaging inflammatory diseases with neutrophil-specific technetium-99m-labeled monoclonal antibody anti-SSEA-1. *J Nucl Med* 1996; 37:1789–1795.
53. Kipper SL, Rypins EB, Evans DG, Thakur ML, Smith TD, Rhodes B. Neutrophil-specific <sup>99m</sup>Tc-labeled anti-CD15 monoclonal antibody imaging for diagnosis of equivocal appendicitis. *J Nucl Med* 2000; 41:449–455.
54. Gratz S, Behr T, Herrmann A, Dresing K, Tarditi L, Franceschini R, Rhodes B, Sturmer KM, Becker W. Intraindividual comparison of <sup>99m</sup>Tc-labelled anti-SSEA-1 antigranulocyte antibody and <sup>99m</sup>Tc-HMPAO labelled white blood cells for the imaging of infection. *Eur J Nucl Med* 1998; 25: 386–393.
55. Rypins EB, Kipper SL. Scintigraphic determination of equivocal appendicitis. *Am Surg* 2000; 66:891–895.

56. Becker W, Goldenberg DM, Wolf F. The use of monoclonal antibodies and antibody fragments in the imaging of infectious lesions. *Semin Nucl Med* 1994; 24:142–153.
57. Sakahara H, Reynolds JC, Carrasquillo JA, et al. In vitro complex formation and biodistribution of mouse antitumor monoclonal antibody in cancer patients. *J Nucl Med* 1989; 30: 1311–1317.
58. Zoghbi S, Thakur M, Gottschalk A. Selective cell labelling: a potential radioactive agent for labeling of human neutrophils. *J Nucl Med* 1981; 22:32P.
59. Fischman AJ, Pike MC, Kroon D, Fucello AJ, Rexinger D, ten Kate C, Wilkinson R, Rubin RH, Strauss HW. Imaging focal sites of bacterial infection in rats with indium-111-labeled chemotactic peptide analogs. *J Nucl Med* 1991; 32:483–491.
60. Babich JW, Graham W, Barrow SA, et al. Technetium-99m-labeled chemotactic peptides: comparison with indium-111-labeled white blood cells for localizing acute bacterial infection in the rabbit. *J Nucl Med* 1993; 34:2176–2181.
61. Fischman AJ, Rauh D, Solomon H, et al. In vivo bioactivity and biodistribution of chemotactic peptide analogs in nonhuman primates. *J Nucl Med* 1993; 34:2130–2134.
62. Pollak A, Goodbody AE, Ballinger JR, Duncan GS, Tran LL, Dunn-Dufault R, Meghji K, Lau F, Andrey TW, Boxen I, Sumner-Smith M. Imaging inflammation with Tc-99m labelled chemotactic peptides: analogues with reduced neutropenia. *Nucl Med Commun* 1996; 17:132–139.
63. Babich JW, Dong Q, Graham W, Barzana M, Ferrill K, Pike M, Fischman AJ. A novel high affinity chemotactic peptide antagonist for infection imaging. *J Nucl Med* 1997; 38:268P.
64. van der Laken CJ, Boerman OC, Oyen WJG, van de Ven MTP, Chizzonite R, Corstens FHM, van der Meer JWM. Preferential localization of systemically administered radiolabeled interleukin-1 $\alpha$  in experimental inflammation in mice by binding to the type II receptor. *J Clin Invest* 1997; 100:2970–2976.
65. van der Laken CJ, Boerman OC, Oyen WJG, van de Ven MTP, van der Meer JWM, Corstens FHM. Imaging of infection in rabbits with radioiodinated interleukin-1 ( $\alpha$  and  $\beta$ ), its receptor antagonist and a chemotactic peptide: a comparative study. *Eur J Nucl Med* 1998; 25:347–352.
66. Barrera P, van Der Laken CJ, Boerman OC, Oyen WJ, van De Ven MT, van Lent PL, van De Putte LB, Corstens FH. Radiolabelled interleukin-1 receptor antagonist for detection of synovitis in patients with rheumatoid arthritis. *Rheumatology* 2000; 39:870–874.
67. Signore A, Chianelli M, Toscano A, et al. A radiopharmaceutical for imaging areas of lymphocytic infiltration,  $^{123}\text{I}$ -interleukin-2 labeling procedure and animal studies. *Nucl Med Commun* 1992; 13:713–722.
68. Chianelli M, Signore A, Fritzberg AR, Mather SJ. The development of technetium-99m-labelled interleukin-2: a new radiopharmaceutical for the in vivo detection of mononuclear cell infiltrates in immune-mediated diseases. *Nucl Med Biol* 1997; 24:579–586.
69. Signore A. Interleukin-2 scintigraphy: an overview. *Nucl Med Commun* 1999; 20:938.
70. Signore A, Chianelli M, Annovazzi A, Rossi M, Maiuri L, Greco M, Ronga G, Britton KE, Picarelli A. Imaging active lymphocytic infiltration in coeliac disease with iodine-123-interleukin-2 and the response to diet. *Eur J Nucl Med* 2000; 27:18–24.
71. Signore A, Chianelli M, Annovazzi A, Bonanno E, Spagnoli LG, Pozzilli P, Pallone F, Biancone L.  $^{123}\text{I}$ -interleukin-2 scintigraphy for in vivo assessment of intestinal mononuclear cell infiltration in Crohn's disease. *J Nucl Med* 2000; 41:242–249.
72. Hay RV, Skinner RS, Newman OC, Kunkel SL, Lyle LR, Shapiro B, Gross MD. Scintigraphy of acute inflammatory lesions in rats with radiolabelled recombinant human interleukin-8. *Nucl Med Commun* 1997; 18:367–378.
73. Gross MD, Shapiro B, Skinner RS, Shreve P, Fig LM, Hay RV. Scintigraphy of osteomyelitis in man with human recombinant interleukin-8. *J Nucl Med* 1996; 37:25P.
74. Rennen HJMM, Boerman OC, Oyen WJG, van der Laken CJ, Corstens FHM. Specific and rapid scintigraphic detection of infection with Tc-99m-labeled interleukin-8. *J Nucl Med* 2001 (in press).
75. Moyer BR, Vallabhajosula S, Lister-James J, Bush LR, Cyr JE, Snow DA, Bastidas D, Lipszyc H, Dean RT. Technetium-99m-white blood cell-specific imaging agent developed from platelet factor 4 to detect infection. *J Nucl Med* 1996; 37:673–679.
76. Palestro CJ, Tomas MB, Bhargava KK, Afriyie MO, Nicodemus CF, Lister-James J, Dean RT. Tc-99m P483H for imaging infection: phase 2 multicenter trial results. *J Nucl Med* 1999; 40:15P.
77. Keelan E, Chapman P, Binns R, Peters A, Haskard D. Imaging vascular endothelial activation: an approach using radiolabeled monoclonal antibodies against the endothelial cell adhesion molecule E-selectin. *J Nucl Med* 1994; 35:276–281.
78. Jamar F, Chapman PY, Harrison AA, Binns RM, Haskard DO, Peters AM. Inflammatory arthritis: imaging of endothelial cell activation with an In-111 labeled F(ab') $_2$  fragment of anti-E-selectin monoclonal antibody. *Radiology* 1995; 194:843–850.
79. Bhatti M, Chapman P, Jamar F, et al. Immunolocalization of active inflammatory bowel disease (IBD) using a monoclonal antibody against E-selectin. *J Nucl Med* 1996; 37 Suppl 5: 114P.
80. Chapman PT, Jamar F, Keelan ET, Peters AM, Haskard DO. Use of a radiolabeled monoclonal antibody against E-selectin for imaging of endothelial activation in rheumatoid arthritis. *Arthritis Rheum* 1996; 39:1371–1375.
81. Jamar F, Chapman PT, Manicourt DH, Glass DM, Haskard DO, Peters AM. A comparison between  $^{111}\text{In}$ -anti-E-selectin mAb and  $^{99\text{m}}\text{Tc}$ -labelled human non-specific immunoglobulin in radionuclide imaging of rheumatoid arthritis. *Br J Radiol* 1997; 70:473–481.
82. Vinjamuri S, Hall AV, Solanki KK, et al. Comparison of  $^{99\text{m}}\text{Tc}$  Infecton imaging with radiolabelled white-cell imaging in the evaluation of bacterial infection. *Lancet* 1996; 347:233–235.
83. Hall AV, Solanki KK, Vinjamuri S, Britton KE, Das SS. Evaluation of the efficacy of  $^{99\text{m}}\text{Tc}$ -Infecton, a novel agent detecting sites of infection. *J Clin Pathol* 1998; 51:215–219.
84. Welling MM, Hiemstra PS, van den Barselaar MT, Paulusma-Annema A, Nibbering PH, Pauwels EKJ, Calame W. Antibacterial activity of human neutrophil defensins in experimental infections in mice is accompanied by increased leukocyte accumulation. *J Clin Invest* 1998; 102:1583–1590.
85. Welling MM, Nibbering PH, Paulusma-Annema A, Hiemstra PS, Pauwels EK, Calame W. Imaging of bacterial infections with  $^{99\text{m}}\text{Tc}$ -labeled human neutrophil peptide-1. *J Nucl Med* 1999; 40:2073–2080.
86. O'Doherty MJ. PET in oncology. I. Lung, breast, soft tissue sarcoma. *Nucl Med Commun* 2000; 21:224–229.
87. Nunan TO, Hain SF. PET in oncology. II. Other tumours. *Nucl Med Commun* 2000; 21:229–233.

88. Warburg O. *On the origin of cancer cells. The metabolism of tumors*. New York: Richard R. Smith; 1931:129–169.
89. Strauss LG. Fluorine-18 deoxyglucose and false-positive results: a major problem in the diagnostics of oncological patients. *Eur J Nucl Med* 1996; 23:1409–1415.
90. Tahara T, Ichiya Y, Kuwabara Y, Otsuka M, Miyake Y, Gunasekera R, Masuda K. High [ $^{18}\text{F}$ ]-fluorodeoxyglucose uptake in abdominal abscesses: a PET study. *J Comput Assist Tomogr* 1989; 13:829–831.
91. Ichiya Y, Kuwabara Y, Sasaki M, Yoshida T, Akashi Y, Murayama S, Nakamura K, Fukumura T, Masuda K. FDG-PET in infectious lesions: the detection and assessment of lesion activity. *Ann Nucl Med* 1996; 10:185–191.
92. O'Doherty MJ, Barrington SF, Campbell M, Lowe J, Bradbeer CS. PET scanning and the human immunodeficiency virus-positive patient. *J Nucl Med* 1997; 38:1575–1583.
93. Guhlmann A, Brecht-Krauss D, Suger G, Glatting G, Kotzerke J, Kinzl L, Reske SN. Chronic osteomyelitis: detection with FDG PET and correlation with histopathologic findings. *Radiology* 1998; 206:749–754.
94. Sugawara Y, Braun DK, Kison PV, Russo JE, Zasadny KR, Wahl RL. Rapid detection of human infections with fluorine-18 fluorodeoxyglucose and positron emission tomography: preliminary results. *Eur J Nucl Med* 1998; 25:1238–1243.
95. Guhlmann A, Brecht-Krauss D, Suger G, Glatting G, Kotzerke J, Kinzl L, Reske SN. Fluorine-18-FDG PET and technetium-99m antigranulocyte antibody scintigraphy in chronic osteomyelitis. *J Nucl Med* 1998; 39:2145–2152.
96. Zhuang H, Duarte PS, Pourdehand M, Shnier D, Alavi A. Exclusion of chronic osteomyelitis with F-18 fluorodeoxyglucose positron emission tomographic imaging. *Clin Nucl Med* 2000; 25:281–284.
97. Kalicke T, Schmitz A, Risse JH, Arens S, Keller E, Hansis M, Schmitt O, Biersack HJ, Grunwald F. Fluorine-18 fluorodeoxyglucose PET in infectious bone diseases: results of histologically confirmed cases. *Eur J Nucl Med* 2000; 27:524–528.
98. Stumpe KD, Dazzi H, Schaffner A, von Schulthess GK. Infection imaging using whole-body FDG-PET. *Eur J Nucl Med* 2000; 27:822–832.